Contents

We are grateful to the reviewer for the thoughtful comments on the manuscript. Our point-to-point responses to each comment are as follows (reviewer comments are in black, our responses are in blue, and revised texts that appear in the manuscript are in quotes and underlined).

Comments:

General Comments:

The article entitled "Organosulfates in atmospheric aerosols in Shanghai, China: seasonal and interannual variability, origin, and formation mechanisms" by Wang et al., presents the OS that are quantified across the 4 seasons in 2015/2016 and 2018/2019, before and after reduction of anthropogenic pollution in the Eastern China, giving valuable insights to their formation mechanisms. They have shown that Ox level (O_3+NO_2) plays a key role in OS formation particularly in summer, while sulfate, aerosol acidity, ALWC are also important factors. Overall, this study is well executed, and the article is well written. The authors have provided sufficient evidence to support their results and conclusions. I recommend acceptance of this manuscript after minor revision listed below.

Specific Comments:

Line 21: Indicate the reason for the observed decrease in OM in 2018/2019 with compared to 2015/2016 upfront

Response: we have indicated the reason for the decrease in OM in the revised manuscript.

"We find that while the concentration of organic aerosol (OA) decreased by 29% from 2015/2016 to 2018/2019, mainly a result of the reduction in anthropogenic pollutant emissions in eastern China, the annually averaged concentrations of 35 quantified OS were overall similar in two years"

Line 22: Indicate percent contribution of OS to OA in 2015/2016 and 2018/2019 next to their average concentrations

Response: We have added the percent contribution of OS to OA in 2015/2016 and 2018/2019, i.e., 0.57%±0.56% and 0.66%±0.56%, respectively, to the revised manuscript.

Line 24, 29-30, 32-34: Is this the average contribution (%) in 2015/2016 and 2018/2019 of each species? If yes, indicate it clearly here as well as in the main text

Response: Yes, there are average contributions. We have clearly indicated this in both the abstract and the main text.

Line 55-56: Replace POM with FPOM to denote "fine particulate organic mass"

Response: We have revised this.

Section 2.1: Give the coordinates of the sampling site

Response: We have added the coordinates (31.201ºN, 121.429ºE) of the sampling site to the revised manuscript.

Line 137: Indicate the temperature at which the sonication took place

Response: The temperature of the sonication bath was maintained at 4 ℃. We have indicated this in the revised manuscript.

Line 140: Indicate time and speed of centrifugation. Also include the model of the centrifuge used

Response: We have included this information in the revised manuscript by rephrasing the sentence here.

"The resulting extracts were mixed with ultrapure water (milliQ, 18.2 M·cm) of the same volume and then centrifuged at 12000 rpm and 4 ℃ for 20 min using a centrifuge (Cence, TGL-16M) to get supernatant for analysis."

Line 145-147: Revise water as (A) and methanol as (B) to match with the gradient elution procedure, as in reversed phase separation starts with high aqueous and then elution progressed with increasing organic mobile phase

Response: Thanks for the suggestion. We have revised this.

Line 155: Indicate why the purities of LAS and GAS are very low.

Response: Because LAS and GAS which are C_2-C_3 OSs are too small, we were not able to find a promising stain and use thin layer chromatography (TLC) on silica gel to purify these standards. Instead, we employed ^{1}H NMR and internal standards to determine their purities.

We have added above sentences to the revised manuscript.

Line 153-158: Indicate the chemical formula of all the standards in parentheses next to their names

Response: We have added the chemical formulas of all the standards, i.e., glycolic acid sulfate (GAS, $C_2H_3O_6S^-$), lactic acid sulfate ($C_3H_5O_6S^-$), limonaketone sulfate ($C_9H_{15}O_6S^-$), α-pinene sulfate ($C_{10}H_{17}O_5S^-$), methyl sulfate ($CH_3O_4S^-$), octyl sulfate ($C_8H_{17}O_4S^-$), and phenyl sulfate ($C_6H_5O_4S^-$).

Section 2.3: Add table S3 to section "2.3 Auxiliary measurements" and change the order of table S2 and S3 in the SI and throughout the main text

Response: We have revised this.

Line 186: Indicate the spike concentration/s

Response: We have added the spike concentrations to Table S2.

Line 187: Indicate that in addition to these standards d-carene sulfate, b-caryophyllene sulfate, camphor sulfate were also used in QC.

Response: We have indicated this by rephrasing the following sentence in the manuscript.

"The extraction efficiency of OS species in filter samples was evaluated by measuring the recovery of ten different OS standards (see Table S2)."

Line 191-193: Indicate briefly how the matrix effect is evaluated for those that were already present in the samples, whether the response is neglected if it is very small compared to the spike concentration or subtracted from the total (sample + standard) before calculating the ratio

Response: As for the standards that were already present in the samples, we subtracted the response in the sample from the total (sample + standard) before calculating the ratio. We have added this statement to the manuscript.

Line 148: Indicate the ESI source was operated in negative ion mode

Response: We have indicated this in the following sentence.

"The ESI source was operated in the negative ion mode under optimum conditions as follows…"

Line 230: Is it high MW CHOS (>400 Da?) or high MW S-containing compounds (>400 Da? CHOS+CHONS) and what is the size range?

Response: It is CHOS in the mass range of 400-700 Da. We have revised "The high-MW CHOS species…" as "The high-MW CHOS species (400-700 Da)…".

Line 231: Indicate what anthropogenic sources

Response: The high-MW CHOS (400-700 Da) consists of a bunch of compounds, and the major ones are listed in Table S4. These species showed a large abundance in winter than in summer, indicating that they were more likely to arise from anthropogenic sources than biogenic emissions. However, the specific anthropogenic sources are currently unclear and need to be further studied.

Line 246: What about $C_{27}H_{53}O_{11}S^-$?

Response: We have performed MS^2 analysis for $C_{27}H_{53}O_{11}S^-$ and found that this species basically did not produce sulfur-containing fragments even under the maximum collision energy (50 eV). We have also noticed that the ion signal originally assigned to $C_{27}H_{53}O_{11}S^-$ is also consistent with a sulfur-free ion ($C_{30}H_{49}O_{11}^-$) with a relative mass error of 4.3 ppm, which is only slightly larger than the mass error for $C_{27}H_{53}O_{11}S^-$ (-1.5 ppm). Therefore, we now do not consider this species to be an organosulfate (it may

not even be a sulfur-containing organic compound) and exclude it from the analysis and discussion in the manuscript.

Line 255-256: Revise the sentence "The quantified OS and NOS accounted for 14-18% and 47-67% by intensity of identified CHOS and CHONS, respectively, in polluted winter days and 15-37% and 58-87%, respectively, in polluted summer days (Fig. 3c)." to read "The quantified OS and NOS accounted for 14-18% and 47-67% by intensity of identified CHOS and CHONS in polluted winter days and 15-37% and 58-87%, in polluted summer days (Fig. 3c), respectively."

Response: Thanks. We have revised this.

Line 274: Replace the values of quantified OS in Centreville, AL using the values given in Hettiyadura et al., 2019 and revise the sentence accordingly

Response: We have replaced values and revised the sentence accordingly.

"…but significantly lower than those observed in Atlanta (2366.4 ng m^{-3}, 16.5% of OC) and Centreville, AL (812 ng m^{-3}, 7.3% of OC) (Hettiyadura et al., 2019)…"

Line 274-275: OC%, instead of OM% is given in Hettiyadura et al. indicate it as follows e.g Atlanta, GA (2366.4 ng m-3, 16.5% of OC) (Hettiyadura et al., 2019)

Response: Thanks. We have revised this.

Line 314-316: Also add Chen et al., 2020, which gives evidence for formation of m/z 211 and 213 from 2-MT-OS

Response: We have added this reference to the manuscript.

Section 3.4: How well the OS correlates with individual Ox species (O$_3$ and NO$_2$ separately)?

Response: The OS showed a correlation with NO$_2$ in all seasons (r=0.40 in spring, autumn and winter, and r=0.60 in summer), but it was correlated well with O$_3$ only in summer (r=0.73 in summer and r=0.19 in other seasons), likely because of the strong titration of O$_3$ by NO in spring, autumn, and winter when the solar radiation (and photochemistry) was relatively weak.

Line 416-421: I suggest also discussing this result in the context of "Multiphase buffer theory explains contrasts in atmospheric aerosol acidity" by Zheng et al, Science, 2020 (https://science.sciencemag.org/content/369/6509/1374)

Response: Thanks for the suggestion. We have added the following discussions to the manuscript.

"A recent study by Zheng et al. (2020) has suggested that aerosol pH levels in populated continental regions including eastern and northern China are widely buffered by ammonium/ammonia, where the variation in aerosol pH is mainly driven by the variation in ALWC and temperature. Therefore, we infer that the lower aerosol pH in summer than in other seasons in Shanghai was mainly a result of decreased ALWC (Figs. 5 and 6c, d) and enhanced temperature (Fig. 2a)."

Tables and Figures

Figure 1: Indicate the coordinates of the sampling site

Response: We have added the coordinates of the sampling site to the figure.

Figure 1: Increase the symbol size of sampling site or use a star to show the sampling site

Response: We have used a star to show the sampling site.

Figure 2 and 4: Indicate the 4 seasons in the time series either in the figure or in the caption

Response: We have indicated the four seasons in both figures.

Figure 2: Indicate the whole Y axis scale of [H+] concentration in scientific notation (10-x..)

Response: We have revised this.

Figure 5: Indicate what is Ox in the figure caption

Response: We have replaced "the O_x concentration" with "the concentration of O_x ($O_x = O_3 + NO_2$)" in the figure caption.

Figure S1: Indicate collision energy of each

Response: The collision energy was 6-10 eV for $C_5H_8NO_8S^-$, 12-25 eV for $C_3H_5O_4S^-$, $C_2H_3O_5S^-$, $C_4H_5O_5S^-$, and $C_{10}H_{16}NO_{10}S^-$, 20-50 eV for $C_6H_5O_4S^-$, and 10-35 eV for the rest. We have added the collision energy of each OS to the figure caption.

Figure S1: Revise the caption to indicate that the S-containing fragments are labeled or label all the fragment ions

Response: We have revised the figure caption as "Figure S1. The MS^2 spectra of quantified OS with the S-containing fragments being labeled."

Table 1: Add retention times

Response: We have added retention times of quantified OS to the table.

Table S1: Indicate the spike concentration/s

Response: We have added spike concentrations to the table

Table S1: Add spike recoveries of LAS and GAS

Response: We have added recoveries of LAS (72.5%) and GAS (77.8%) to the table

Table S2: Clearly indicate the spike concentration of individual OS and/or add the information presented in the table caption to the table

Response: We have added the spike concentration of individual OS, as well as concentrations of OM, NO_3^-, SO_4^{2-}, and OS ambient aerosol samples to the table.

Table S2: Indicate the dates of the samples used

Response: We have indicated the dates of the samples in the table.

Technical corrections

Table 1: Adjust the column width to indicate anthropogenic in one line

Response: We have revised this.

Line 86, 138, 142, 144: Define all acronyms where it first appears (OM, PTFE, UPLC, BEH...)

Response: We have revised this.

Line 116: PRD should be corrected as YRD

Response: Thanks, we have corrected it.

Line 144: Add 'Waters' in parentheses

Response: We have revised this.

Line 169: Organic matter is already defined at line 86, use acronym

Response: We have used acronym here.

Line 288: Correct "$(C_7H_9O_7S)$" as "$(C_7H_9O_7S^-)$"

Response: We have corrected it.

Line 297: Use 2-MA-OS, as the acronym is introduced before
Use acronyms consistently e.g. OS_i instead of OSI (line 394) and Ox or Ox (subscripted) consistently
Add GA after Atlanta and AL after Centreville (e.g. Atlanta, GA and Centreville, AL)

Response: We have corrected all of these technical issues.

Response to Reviewer #3

We are grateful to the reviewer for their thoughtful comments on the manuscript. Our point-to-point responses to each comment are as follows (reviewer comments are in black, our responses are in blue, and revised texts that appear in the manuscript are in quotes and underlined).

Comments:

General Comments:

This manuscript presents a comprehensive characterization of the seasonality and interannual variability of the abundance, sources, and formation processes of organosulfates (OS) in ambient aerosols in Shanghai, China. The authors found that the contribution of OS to organic aerosols (OA) has increased obviously in recent years and that biogenic emissions such as isoprene and monoterpenes contributed significantly to the production of OS and SOA in this polluted region. The authors also found that the production of OS was largely controlled by atmospheric oxidizing capacity (i.e., Ox level), and inferred that the mitigation of Ox pollution can effectively reduce the production of OS and SOA in eastern China. In general, the measurements are well done, the manuscript is nicely written, and the results are properly discussed. This work adds new understandings of the characteristics and mechanisms of OS formation in polluted atmosphere. I recommend its publication in ACP after considering the following concerns.

Specific comments:

L230-231. The authors stated that the high-molecular-weight CHOS species are likely to arise from anthropogenic sources. What are the molecular identities of these species? Are they accretion reaction products of smaller CHOS species?

Response: We have listed the molecular formulas of high-molecular-weight CHOS species in Table S4. We found that although several species had two sulfur atoms, which may be accretion reaction products of smaller CHOS species, most of them only had one sulfur atom.

Table S4. The molecular formulas of high-molecular-weight CHOS species observed during the pollution periods of winter and summer in 2019.

Winter in 2019		Summer in 2019	
Formula	m/z	Formula	m/z
$C_{18}H_{33}O_8S^-$	409.1896	*$C_{18}H_{13}O_8S_2^-$	421.0052
$C_{20}H_{37}O_7S^-$	421.226	$C_{22}H_{21}O_7S^-$	429.1008
$C_{19}H_{37}O_8S^-$	425.2209	$C_{14}H_{13}O_{14}S^-$	437.0026
$C_{22}H_{43}O_6S^-$	435.278	$C_{15}H_{15}O_{14}S^-$	451.0183
*$C_{16}H_{23}O_{10}S_2^-$	439.0733	$C_{15}H_{17}O_{14}S^-$	453.0339
$C_{18}H_{31}O_{10}S^-$	439.1638	*$C_{15}H_{19}O_{12}S_2^-$	455.0318
$C_{24}H_{37}O_8S^-$	485.2209	$C_{15}H_{15}O_{15}S^-$	467.0132
$C_{30}H_{27}O_{12}S^-$	611.1223	$C_{24}H_{37}O_8S^-$	485.2209
$C_{37}H_{49}O_7S^-$	637.3199	$C_{34}H_{49}O_5S^-$	569.3301
$C_{31}H_{57}O_{14}S^-$	685.3469	$C_{35}H_{53}O_6S^-$	601.3563
		$C_{36}H_{47}O_6S^-$	607.3093
		$C_{37}H_{49}O_7S^-$	637.3199
		$C_{37}H_{59}O_7S^-$	647.3981
		$C_{43}H_{63}O_5S^-$	691.4396

*The high-molecular-weight CHOS species with two sulfur atoms may be accretion products of smaller CHOS species.

Sect. 3.3 and Table 1. Some of quantified OS species may have one or more structural isomers. Have all the isomers been considered in quantification? If so, information regarding the number of isomers and their retention times for each OS species should be provided.

Response: All the isomers were considered in quantification and we have added the retention times for each isomer to Table 1.

L360-361. The authors claimed that the abundance of anthropogenic OS decreased in 2018/2019 compared to that in 2015/2016. However, only a tiny portion of anthropogenic OS have been quantified

in this study. Therefore, care must be taken when making conclusions regarding the inter-annual variation of the formation of anthropogenic OS.

Response: Thanks for the suggestion. We have rephrased the statement in L360-363.

"Although the concentration of quantified OS$_a$ decreased in 2018/2019, we are not sure whether the total concentration of OS$_a$ decreased because only a small fraction of OS$_a$ were quantified. The inter-annual variations of OS$_a$ warrants further studies."

L368-369. Further discussions regarding the origin of phenyl sulfate and benzyl sulfate may need to be added. For example, a recent study by Huang et al. (ES&T, 2020) found that phenyl sulfate and benzyl sulfate can also be produced by sulfate radical-initiated aqueous-phase oxidation of aromatic compounds.

Response: We have added further discussions regarding the origin of phenyl and benzyl sulfate to the manuscript.

"Phenyl sulfate and benzyl sulfate may be produced by photooxidation of naphthalene and 2-methylnaphthalene (Riva et al., 2015) and/or sulfate radical reaction with aromatic compounds such as benzoic acid and toluene in the aqueous phase (Huang et al., 2020)"

Fig. 5. The authors may plot the averages of OS concentrations within regular Ox or ALWC intervals in the figure to better demonstrate the trends of OS vs. Ox and OS vs. ALWC.

Response: We have added the averages of OS concentrations within regular Ox or ALWC intervals (every ten unit-length) in the figure.
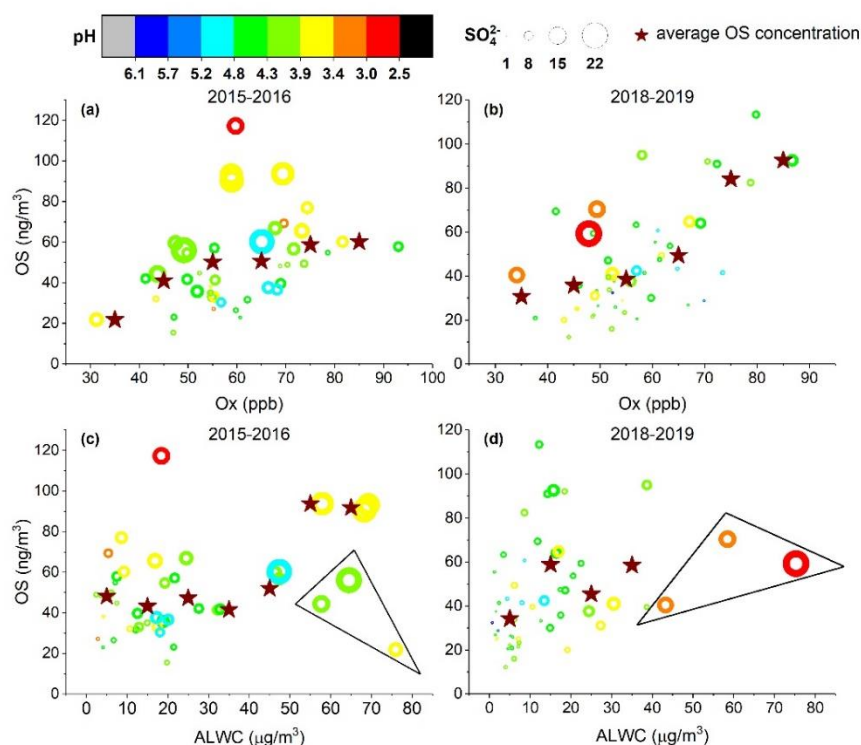
Changes made in the manuscript

Line 20: Define UPLC-ESI-QToF-MS as "ultra-performance liquid chromatography quadrupole time-of-flight mass spectrometer equipped with an electrospray ionization (ESI) source".

Line 23: Indicate the reason for the decrease in OM: "mainly a result of the reduction in anthropogenic pollutant emissions in eastern China".

Line 25: Add the percent contribution of OS to OA in 2015/2016 and 2018/2019.

Line 146: Add "centrifugated at 12000 rpm and 4 °C for 20 min using a centrifuge (Cence, TGL-16M)".

Line 160-162: Add a statement "Because LAS and GAS are too small in molecular size, we could not find a promising stain and use thin layer chromatography (TLC) on silica gel to purify them. Instead, we employed ^{1}H NMR and an internal standard (dichloroacetic acid) to determine their puritiesThe purities of (8% for GAS and 15% for LAS)".

Line 177: Add a sentence "The seasonal and annual average values of meteorological parameters and concentrations of trace gases, PM$_{2.5}$ and its major components in 2015/2016 and 2018/2019 are listed in Table S1".

Line 197: Add recoveries for Lactic acid sulfate and Glycolic acid sulfate.

Line 202: Add a statement "As for the standards that were already present in the samples, we subtracted the response in the sample from the total (sample + standard) before calculating the ratio".

Line 267: Revise the sentence to read "The quantified OS and NOS accounted for 14-18% and 47-67% by intensity of identified CHOS and CHONS in polluted winter days and 15-37% and 58-87%, in polluted summer days (Fig. 3c), respectively".

Line 377: Add a statement "Although the concentration of quantified OS$_a$ decreased in 2018/2019, we are not sure whether the total concentration of OS$_a$ decreased because only a small fraction of OS$_a$ were quantified. The inter-annual variations of OS$_a$ warrants further studies".

Line 387: Add "…and/or sulfate radical reaction with aromatic compounds such as benzoic acid and toluene in the aqueous phase (Huang et al., 2020)".

Line 437: Add a discussion "A recent study by Zheng et al. (2020) has suggested that aerosol pH levels in populated continental regions including eastern and northern China are widely buffered by ammonium/ammonia, where the variation in aerosol pH is mainly driven by the variation in ALWC and temperature. Therefore, we infer that the lower aerosol pH in summer than in other seasons in Shanghai was mainly a result of decreased ALWC (Figs. 5 and 6c, d) and enhanced temperature (Fig. 2a)".

Revise figures and tables and correct technical issues suggested by the reviewers.

Manuscript file with track changes

Organosulfates in atmospheric aerosols in Shanghai, China: seasonal and interannual variability, origin, and formation mechanisms

Yao Wang[1], Yue Zhao[1,2,*], Yuchen Wang[3], Jian-Zhen Yu[3,4], Jingyuan Shao[5], Ping Liu[1], Wenfei Zhu[1], Zhen Cheng[1], Ziyue Li[1], Naiqiang Yan[1,2], Huayun Xiao[1]

[1]School of Environmental Science and Engineering, Shanghai Jiao Tong University, Shanghai 200240, China

[2]Shanghai Institute of Pollution Control and Ecological Security, Shanghai 200092, China

[3]Division of Environment & Sustainability, Hong Kong University of Science & Technology, Hong Kong, China

[4]Department of Chemistry, Hong Kong University of Science & Technology, Hong Kong, China

[5]College of Flight Technology, Civil Aviation University of China, Tianjin 300300, China

*Corresponding author: Yue Zhao (yuezhao20@sjtu.edu.cn)

Abstract

Organosulfates (OS) are ubiquitous in the atmosphere and serve as important tracers for secondary organic aerosols (SOA). Despite intense research over years, the abundance, origin, and formation mechanisms of OS in ambient aerosols, in particular in regions with severe anthropogenic pollution, are still not well understood. In this study, we collected filter samples of ambient fine particulate matter ($PM_{2.5}$) over four seasons in both 2015/2016 and 2018/2019 at an urban site in Shanghai, China, and comprehensively characterized the OS species in these $PM_{2.5}$ samples using an ultra-performance liquid chromatography quadrupole time-of-flight mass spectrometer equipped with an electrospray ionization (ESI) source liquid chromatography coupled to a high resolution mass spectrometer (UPLC-ESI-QToF-MS). We find that while the concentration of organic aerosol (OA) decreased by 29% in 2018/2019, compared to that in 2015/2016, mainly a result of the reduction in anthropogenic pollutant emissions in eastern China, the annually averaged concentrations of 35 quantified OS were overall similar in two years (65.5 ± 77.5 ng m^{-3}, $0.57\%\pm0.56\%$ of OA in 2015/2016 versus 59.4 ± 79.7 ng m^{-3}, $0.66\%\pm0.56\%$ of OA in 2018/2019), suggesting an increased contribution of SOA to OA in 2018/2019 than in 2015/2016. Isoprene- and monoterpene-derived OS are the two most abundant OS families, on average accounting for 36.3% and 31.0% of the quantified OS concentrations, respectively, during the two sampling years, suggesting an important contribution of biogenic emissions to the production of OS and SOA in Shanghai. The abundance of biogenic OS, particularly those arising from isoprene, exhibited strong seasonality (peaked in summer) but no significant interannual variability. In contrast, the quantified anthropogenic OS such as diesel-derived ones had little seasonal variability and declined obviously in 2018/2019 compared with that in 2015/2016. This reflects a significant change in precursor emissions in eastern China in recent years. The C_2/C_3 OS species that have both biogenic and anthropogenic origins averagely contributed to 19.0% of the quantified OS, with $C_2H_3O_6S^-$, $C_3H_5O_5S^-$, and $C_3H_5O_6S^-$ being the most abundant ones, together accounting for 76% of C_2/C_3 OS concentrations in 2015/2016 and 2018/2019. 2-Methyltetrol sulfate (2-MT-OS, $C_5H_{11}O_7S^-$) and monoterpene-derived $C_{10}H_{16}NO_7S^-$ were the most abundant OS and nitrooxy-OS in summer, on average contributing to 31% and 5% of the quantified OS, respectively, during the summertime of the two sampling years. The substantially larger concentration ratio of 2-MT-OS to 2-methylglyceric acid sulfate (2-MA-OS, $C_4H_7O_7S^-$) in summer (6.8-7.8) than in other seasons (0.31-0.78) implies that low-NO$_x$ oxidation pathways played a dominant role in isoprene-derived SOA formation in summer, while high-NO$_x$ reaction pathways were more important in other seasons. We further find that the production of OS was largely controlled by the level of O$_x$ (O$_x$ = O$_3$ + NO$_2$), namely, the photochemistry of OS precursors, in particular in summer, though sulfate concentration, aerosol acidity, as well as aerosol liquid water content (ALWC) that could affect the heterogeneous chemistry of reactive intermediates leading to OS formation also played a role. Our study provides valuable insights into the characteristics and mechanisms of OS formation in a typical Chinese megacity and implies that mitigation of O$_x$ pollution can effectively reduce the production of OS and SOA in eastern China.

1 Introduction

Secondary organic aerosol (SOA) accounts for a significant fraction of atmospheric fine particulate matter ($PM_{2.5}$) (Jimenez et al., 2009; Huang et al., 2014) and contributes significantly to deteriorated air quality and Earth's climate forcing (Ramanathan et al., 2001; Mahowald, 2011; Shrivastava et al., 2017; Huang et al., 2014). SOA consists of thousands of organic compounds that are diverse in molecular properties. Identification and quantification of the composition of SOA are essential for understanding the composition, the chemistry of formation and evolution, properties, and climate and health impacts of SOA (Hoffmann et al., 2011; Noziere et al., 2015). However, currently only a small portion of organic matters in SOA are identified as specific compounds (Hoffmann et al., 2011; Noziere et al., 2015; Johnston and Kerecman, 2019). Organosulfates (OS) are important constituents of SOA and have been frequently detected in both polluted and clean environments (Iinuma et al., 2007a; Surratt et al., 2008; Claeys et al., 2010; Stone et al., 2012; Hansen et al., 2014; Kourtchev et al., 2016; Froyd et al., 2010; Hawkins et al., 2010; Hatch et al., 2011; Hettiyadura et al., 2019; Wang et al., 2019a; Le Breton et al., 2018; Wang et al., 2018; Huang et al., 2018; Hettiyadura et al., 2017; Wang et al., 2016b; Meade et al., 2016; Liao et al., 2015; Shakya and Peltier, 2015; Ma et al., 2014; Tao et al., 2014; He et al., 2014; Lin et al., 2012a). It has been estimated that OS accounted for 6-12% of total sulfur in a rural area in K-puszta, Hungary (Lukacs et al., 2009), 1.3% of fine particulate organic mass (FPOM) in Fairbanks, Alaska (Shakya and Peltier, 2013), and 1-13% of ~~fine~~ FPOM across the continental United States (Tolocka and Turpin, 2012; Shakya and Peltier, 2015). Studies have also shown that OS can affect aerosol properties such as acidity, viscosity, hygroscopicity, and light-absorbing properties (Nguyen et al., 2012; Hansen et al., 2015; Estillore et al., 2016; DeRieux et al., 2018; Fleming et al., 2019; Riva et al., 2019; Olson et al., 2019).

Chamber studies have revealed that OS can originate from the (photo)oxidation of both biogenic precursors such as isoprene (Gomez-Gonzalez et al., 2008; Surratt et al., 2007b; Surratt et al., 2007a), monoterpenes (Iinuma et al., 2007a; Surratt et al., 2007a; Surratt et al., 2008; Iinuma et al., 2007b; Iinuma et al., 2009), sesquiterpenes (Chan et al., 2011), and 2-methyl-3-buten-2-ol (Zhang et al., 2012), as well as anthropogenic precursors such as polycyclic aromatic hydrocarbons, long-chain alkanes, naphthenes (Riva et al., 2015; Riva et al., 2016b), and diesel and biodiesel fuel vapors (Blair et al., 2017) in the presence of sulfate aerosol or SO_2. Many of OS observed in these chamber studies have also been detected in ambient atmosphere, among which isoprene- and monoterpene-derived OS are usually most abundant in forested, rural, and even urban areas (Stone et al., 2012; Ma et al., 2014; Meade et al., 2016; Hettiyadura et al., 2019; Kourtchev et al., 2016; Kristensen and Glasius, 2011; Wang et al., 2019a; He et al., 2014; Hatch et al., 2011; Surratt et al., 2008; Hettiyadura et al., 2017).

In addition to the precursors, detailed formation mechanisms of OS have also been widely studied. The acid-catalyzed ring-opening reaction of epoxides was established to be an important mechanism for the formation of OS (Surratt et al., 2010; Lin et al., 2012b; Iinuma et al., 2009; Zhang et al., 2014), in particular for isoprene-derived OS (Surratt et al., 2010; Lin et al., 2012b; Hatch et al., 2011). 2-Methyltetrol sulfate (2-MT-OS, $C_5H_{11}O_7S^-$), formed via reactive uptake of isoprene epoxide (IEPOX) on sulfate, is one of the most abundant OS in atmospheric aerosol (Chan et al., 2010; Liao et al., 2015), which can contribute up to 12.6% of the organic carbon mass in Atlanta, GA (Hettiyadura et al., 2019). Another OS formation pathway is the nucleophilic substitution of tertiary organonitrates by inorganic sulfate. Darer et al. (2011) found that tertiary organonitrates are thermodynamically unstable and can undergo nucleophilic substitution with sulfate to generate OS rapidly.

82   This mechanism can also explain the formation of some nitrooxy-OS (NOS). In atmospheric aqueous phase, sulfate radicals
83   that can be produced by oxidation of S(IV) species in the presence of transition metal ions (TMI) (Grgic et al., 1998; Herrmann,
84   2003) or by OH radical reaction with bisulfate (Herrmann, 2003; Jiang et al., 1992) can also react with unsaturated organic
85   compounds to form OS. Laboratory studies have shown that a large number of OS were produced by the bulk aqueous-phase
86   oxidation of isoprene or its oxidation products, methyl vinyl ketone (MVK) and methacrolein (MACR), in the presence of
87   inorganic sulfate or peroxodisulfate under irradiation (Nozière et al., 2010; Schindelka et al., 2013), or in the presence of S(IV)
88   and TMI under dark conditions (Huang et al., 2019). However, field observational evidence for this mechanism is still lacking.
89   In addition, reactive uptake of SO_2 on organic aerosol can also result in the production of OS. Laboratory studies have found
90   that sulfur dioxide (SO_2) could react with C=C bond in unsaturated fatty acids under dark conditions to form OS (Shang et
91   al., 2016). Such OS have been detected in ambient atmosphere with an estimated contribution of 0.3‰-0.9‰ to OM in $PM_{2.5}$
92   in southern China (Zhu et al., 2019). Recent studies have also shown efficient production of OS from heterogeneous/aqueous-
93   phase reactions of SO_2 with organic peroxide-containing aerosol and SOA (Wang et al., 2019b; Yao et al., 2019). Such OS
94   production was found to be mainly a result of the direct reaction between SO_2 and peroxides, rather than acid-catalyzed
95   reaction involving inorganic sulfate (Wang et al., 2019b). Currently, the acid-catalyzed ring-opening reaction of IEPOX has
96   been the most well-studied mechanism and proved to be important in atmospheric OS formation by both field and modelling
97   studies (Surratt et al., 2010; Kourtchev et al., 2016; Hettiyadura et al., 2019; Hatch et al., 2011; Chan et al., 2010; McNeill et
98   al., 2012; Worton et al., 2013; He et al., 2018; Pye et al., 2013). However, atmospheric importance of other OS formation
99   mechanisms remains to be evaluated.

100 The OS formation pathways aforementioned can be affected by aerosol properties such as acidity, aerosol liquid water content
101 (ALWC), and sulfate concentration. There is ample evidence from laboratory studies that increased aerosol acidity
102 significantly enhances the production of OS from acid-catalyzed reactions (Iinuma et al., 2007b; Chan et al., 2011; Surratt et
103 al., 2007a; Surratt et al., 2007b; Zhang et al., 2012), while field studies have shown that the abundance of OS was not or only
104 weakly correlated with aerosol acidity in some locations (Nguyen et al., 2014; Budisulistiorini et al., 2015; Brüggemann et
105 al., 2017; Rattanavaraha et al., 2017), suggesting the existence of other factors (e.g., ALWC, sulfate content, etc.) that control
106 OS formation in these areas. ALWC has dual effects on OS formation. On one hand, elevated ALWC can reduce the viscosity
107 and/or inhibit the liquid-liquid phase separation of aerosol, which would favor the dissolution and mixing of reactive
108 intermediates such as IEPOX and multifunctional aldehydes in aqueous sulfate aerosol (Shiraiwa et al., 2011; Liao et al., 2015;
109 McNeill et al., 2012) or SO_2 in organic aerosol (Shang et al., 2016; Passananti et al., 2016; Yao et al., 2019), thereby enhancing
110 OS formation. On the other hand, high ALWC would decrease aerosol acidity via dilution, hence inhibiting the acid-catalyzed
111 OS formation. High ALWC may also promote the hydrolysis of OS in aqueous aerosol (Darer et al., 2011).

112 Quantification of OS is important for understanding their abundance and the chemistry of formation and evolution in the
113 atmosphere. Owing to the lack of authentic standards, the quantification of OS remains a challenging task. Recently, several
114 research groups have synthesized a series of authentic standards (e.g., glycolic acid sulfate, lactic acid sulfate, hydroxyacetone
115 sulfate, 2-methyltetrol sulfate, benzyl sulfate, α-pinene sulfate, β-pinene sulfate, and limonene sulfate) that are structurally
116 the same or similar with the OS found in atmospheric aerosols (Kundu et al., 2013; Staudt et al., 2014; Hettiyadura et al.,
117 2015; Wang et al., 2017; Olson et al., 2011; Huang et al., 2018; Budisulistiorini et al., 2015). They used these authentic

118 standards to quantify OS in ambient aerosols and provided important constraints on the abundance, origin, and chemistry of

119 OS in the atmosphere.

120 Up to date, there are few studies characterizing atmospheric OS in areas with severe anthropogenic pollution. Situated in the

121 eastern Yangtze River Delta (~~PRD~~YRD) of China, Shanghai has a population of more than 24 million and is plagued by air

122 pollution (Behera et al., 2015; Wang et al., 2016a). Here we conducted a comprehensive investigation of the molecular

123 composition, abundance, sources, and formation processes of OS in ambient aerosols in Shanghai. More than 150 ambient

124 $PM_{2.5}$ samples collected over four seasons during both 2015/2016 and 2018/2019 in urban Shanghai were analyzed using

125 ~~ultra-performance liquid chromatography quadrupole time-of-flight mass spectrometer (~~UPLC-ESI-QToF-MS~~)~~, and 35 OS

126 were quantified using 7 synthesized and commercially purchased OS standards. Seasonal and interannual variations of OS,

127 in response to the changes in emissions, meteorological conditions, and $PM_{2.5}$ chemical compositions, were comprehensively

128 characterized, and the influencing factors such as aerosol acidity, ALWC, sulfate content, oxidant level and so on for OS

129 formation were probed. This study would help to understand the characteristics and mechanisms of OS and SOA production

130 under the strong influence of anthropogenic pollution in Chinese megacities.

131 **2 Materials and methods**

132 **2.1 Ambient Sample collection**

133 In total 156 ambient $PM_{2.5}$ samples were collected from 8 April 2015 to 16 January 2016 and from 23 October 2018 to 5

134 August 2019 in Shanghai, China. The sampling site is located on the rooftop of a 20-meter-tall teaching building on the Xuhui

135 Campus of Shanghai Jiao Tong University at 31.201^{o}N, 121.429^{o}E, which is in downtown and surrounded by residential and

136 commercial areas (see Fig. 1a, b). There is a main street 230 m east to the sampling site. The $PM_{2.5}$ samples were collected

137 on pre-baked (550 ℃, 8 h) quartz-fiber filters (Whatman) from 9:00 am to 8:00 am of the next day using a high-volume

138 sampler (HiVol 3000, Ecotech) at a flow rate of 67.8 m^3 h^{-1}. The collected samples were wrapped in pre-baked (550 ℃, 8 h)

139 aluminum foil and stored at -20 ℃ before analysis.

140 **2.2 Organosulfate measurement with UPLC-ESI-ToF-MS**

141 An aliquot of ~17 cm^2 was removed from each filter sample and extracted in 3 mL of methanol (LC-MS grade, CNW

142 Technologies GmbH) twice under sonication in an ice bath at 4 ℃ for 30 min. The extracts derived each time were combined

143 and filtered through a 0.45 μm poly tetra fluoroethylene (PTFE) syringe filter (CNW Technologies GmbH) to remove

144 insoluble materials, and subsequently concentrated to 250 μL with a gentle stream of ultra-high-purity nitrogen (Shanghai

145 Likang Gas Co., Ltd). The resulting extracts were mixed with ultrapure water (milliQ, 18.2 MΩ·cm) of the same volume and

146 centrifugated at 12000 rpm and 4 ℃ for 20 min using a centrifuge (Cence, TGL-16M) to get supernatant for analysis.

147 The resulting solutions were analyzed using an Acquity UPLC~~ (~~ (Waters) coupled to a Xevo G2-XS QToF-MS (Waters)

148 having a mass resolving power of ≥ 40000 and equipped with an electrospray ionization (ESI) source. The analytes were

149 separated by a~~n~~ ethylene bridged hybrid (BEH) C_{18} column (2.1×100 mm, 1.7 μm particle size, waters) at 50 ℃. A gradient

150 elution procedure was performed using water (A) and methanol (B)~~methanol (A) and water (B)~~ both containing 0.1% acetic

151 acid (v/v) as the eluents: A was maintained at 99% for 1.5 min, decreased to 46% in 6.5 min and to 5% in 3 min, then decreased

152   to 1% in 1 min and held for 2 min, finally returned to 99% in 0.5 min and held for 1.5 min to equilibrate the column. The total

153   eluent flow rate was 0.33 mL min^{-1} and the sample injection volume was 2.0 μL. The ESI source was operated in the negative

154   ion mode under optimum conditions as follows: capillary voltage 2.0 kV, sampling cone voltage 40 V, source offset voltage

155   80 V, source temperature 115°C, desolvation gas temperature 450°C, cone gas 50 L h^{-1}, desolvation gas 900 L h^{-1}.

156   The quantified OS as well as the authentic and surrogate standards used for the quantification of each OS are listed in Table

157   1. The OS standards were selected by mainly referring to Hettiyadura et al. (2019), which is based upon a comparison of the

158   MS/MS pattern between authentic standards and targeted OS in ambient aerosols, as well as to Wang et al (2018). Glycolic

159   acid sulfate (GAS, $C_2H_3O_6S^-$) and lactic acid sulfate (LAS, $C_3H_5O_6S^-$) were synthesized according to Olson et al. (2011).

160   Because LAS and GAS are too small in molecular size, we could not find a promising stain and use thin layer chromatography

161   (TLC) on silica gel to purify them. Instead, we employed ^{1}H NMR and an internal standard (dichloroacetic acid) to determine

162   their purities~~The purities of~~ (8% for GAS and 15% for LAS). Limonaketone sulfate ($C_9H_{15}O_6S^-$) and α-pinene sulfate

163   ($C_{10}H_{17}O_5S^-$) ~~were synthesized and details were described in Wang et al. (2017). Other OS standards including sodium methyl

164   sulfate ($CH_3O_4S^-$, 99%, Macklin), sodium octyl sulfate ($C_8H_{17}O_4S^-$, 95%, Sigma-Aldrich), and potassium phenyl sulfate

165   ($C_6H_5O_4S^-$, 98%, Tokyo Chemical Industry, Shanghai) were commercially purchased. The quantified OS were also analyzed

166   in tandem mass spectrometry (MS/MS) at a collision energy of 10-50 eV to confirm whether they are OS by sulfur-containing

167   fragment ions observed. In this study, most quantified OS were fragmented to the bisulfate anion (m/z 97) and several

168   quantified OS were only fragmented to the sulfate radical anion (m/z 96) and the sulfite radical anion (m/z 80) (see Fig. S1).

2.3 Auxiliary measurements

170   Meteorological parameters, including temperature, relative humidity (RH), and wind speed (WS) were continuously

171   monitored by Shanghai Hongqiao international airport station, which is 9 km west to the sampling site (Fig. 1c). The

172   concentrations of SO$_2$, nitrogen dioxide (NO$_2$), O$_3$ and PM$_{2.5}$ were measured by a state-controlled air quality monitoring

173   station on the Xuhui Campus of Shanghai Normal University, which is 4.5 km southwest to the sampling site for the PM$_{2.5}$

174   filter samples (Fig. 1c). Organic carbon (OC) and elemental carbon (EC) in PM$_{2.5}$ filter samples were measured by a thermal-

175   optical multiwavelength carbon analyzer (DRI Model 2015). The concentration of OM was derived by multiplying the OC

176   by 1.6 (Tao et al., 2017). Water-soluble inorganic compounds including sulfate, nitrate, chloride, ammonium, potassium, and

177   calcium were analyzed with an ion chromatograph (Metrohm MIC). The seasonal and annual average values of meteorological

178   parameters and concentrations of trace gases, PM$_{2.5}$ and its major components in 2015/2016 and 2018/2019 are listed in Table

179   S1.

2.4 Estimation of aerosol liquid water content and pH

181   The ISORROPIA-II thermodynamic model (Fountoukis and Nenes, 2007) was employed to predict ALWC and aerosol pH.

182   The aerosol water-soluble inorganic ion concentrations, as well as temperature and RH were used as the model input. The

183   model was run in the forward model for metastable aerosol, which was shown to give a more accurate representation of

184   aerosol pH than using the reverse-mode calculations when with only aerosol data input (Guo et al., 2015; Hennigan et al.,

185   2015). ISORROPIA-II calculates the equilibrium concentration of aerosol hydronium ions (H$^+_{air}$) per volume of air (μg m^{-3}),

带格式的：下标
带格式的：下标
带格式的：下标
带格式的：上标
带格式的：下标
带格式的：下标
带格式的：下标
带格式的：上标
带格式的：下标
带格式的：下标
带格式的：下标
带格式的：上标
带格式的：下标
带格式的：下标
带格式的：下标
带格式的：上标
带格式的：下标
带格式的：下标
带格式的：上标
带格式的：下标
带格式的：下标
带格式的：下标
带格式的：上标
带格式的：下标
带格式的：下标
带格式的：下标
带格式的：上标

186 along with ALWC (μg m^{-3}). The aerosol pH was then derived by

$$pH = -\log_{10}\left(H^+_{aq}\right) = -\log_{10}\frac{1000H^+_{air}}{ALWC},\qquad(1)$$

188 where H^+_{aq} is the concentration of hydronium ions in aqueous aerosol (mol L^{-1}). In this study, ALWC associated with organic

189 aerosol and its influences on aerosol pH were not considered. However, previous studies showed that water uptake by organic

190 aerosol only contributed to a minor fraction (5%) of total ALWC and had a negligible influence on aerosol pH in haze events

191 in China (Liu et al., 2017). The seasonally and annually averaged ALWC and aerosol pH levels in 2015/2016 and 2018/2019

192 are also given in Table S1.

2.5 Quality control

194 The extraction efficiency of OS species in filter samples was evaluated by measuring the recovery of ten different OS

195 standards (see Table S2). The synthesized and commercially purchased OS standards were spiked into blank and pre-baked

196 quartz filters, followed by extraction and analysis with the same procedures for ambient samples. The recoveries of OS

197 standards were about 84-94% except for Δ-Carene OS, Lactic acid sulfate, and Glycolic acid sulfate, the recovery of which was

198 66%, 72.5%, and 77.8%, respectively (see Table S2). This result suggests a fairly high extraction efficiency for the majority

199 of OS species in this study.

200 In addition, we evaluated the matrix effect on the signal response of OS by comparing the measured signal intensity of OS

201 standards added to the extracts of ambient PM$_{2.5}$ filter samples with that of pure OS standard solutions. Table S3 gives the

202 ratios of measured signal intensity of OS standards in filter sample extracts to that in pure solutions. As for the standards that

203 were already present in the samples, we subtracted the response in the sample from the total (sample + standard) before

204 calculating the ratio. Most of OS standards had a ratio around 1, suggesting no obvious matrix effect on the measurement of

205 the majority of OS species. However, the two smallest OS standards, methyl sulfate and glycolic acid sulfate that were the

206 very first species eluted from LC column, had a ratio significantly smaller than 1, suggesting the inhibited ionization of these

207 two OS likely by the highly soluble and polar species in the filter samples that were co-eluted with these two OS. We note

208 that the matrix effect for these two OS is dependent on the PM$_{2.5}$ mass loading. For example, the signal ratio of glycolic acid

209 sulfate standard measured in filter sample extracts versus in pure solutions ranged from 0.17-0.31 (Exps. 1-2) for very polluted

210 days to 0.45-0.53 for clean days (Exps. 3-4). This implies that the abundance of glycolic acid sulfate in ambient aerosols

211 reported here may be underestimated by a factor of 2-6 due to the matrix effect.

3 Results and Discussion

3.1 Overview of pollution characteristics during sampling periods

214 Figure 2 shows the time series of meteorological parameters, O$_3$, NO$_2$, SO$_2$, PM$_{2.5}$ and its major components, as well as H^+_{aq}

215 and ALWC during the sampling periods. The average values (concentrations) of each parameter (species) were given in Table

216 S1. The meteorological conditions (wind speed, temperature, and RH) were overall similar in 2015/2016 and 2018/2019.

217 While the NO$_2$ concentration decreased from 27.0$\pm$13.0 ppb in 2015/2016 to 21.3$\pm$10.3 ppb in 2018/2019, the O$_3$ level had

218 no obvious difference in two years (29.8±15.2 ppb in 2015/2016 versus 29.6±13.9 ppb in 2018/2019), consistent with the

219 nonlinear response of O_3 production to precursor emissions (Liu and Wang, 2020). The annual average mass loading of $PM_{2.5}$

220 declined by 34.5% in 2018/2019 (38.6±24.0 μg m^{-3}) compared to that 2015/2016 (59.0±37.9 μg m^{-3}), largely driven by the

221 strong decrease in the abundance of OM (29.1%) and sulfate (37.4%). The decrease of $PM_{2.5}$, OM, and sulfate concentrations

222 from 2015/2016 to 2018/2019 reflects a significant reduction in anthropogenic pollutant emissions in eastern China in recent

223 years. In contrast to OM and sulfate, the concentration of nitrate had little change between 2015/2016 (8.8±8.9 μg m^{-3}) and

224 2018/2019 (8.4±7.8 μg m^{-3}), despite an obvious decrease in NO_2 concentration. This is at least partly a result of reduced

225 aerosol acidity (H^+_{aq}, see Fig. 2 and Table S3S1) and thereby enhanced partitioning of HNO_3 into the particle phase.

226 Furthermore, the nitrate concentration showed a strong seasonality, ranging from 1.0±1.1 and 3.4±3.2 μg m^{-3} in summer to

227 16.6±10.0 and 14.1±10.0 μg m^{-3} in winter in 2015/2016 and 2018/2019, respectively, partly owing to the seasonal variation

228 of temperature and aerosol acidity that modulates the gas/particle partitioning of nitrate (Fisseha et al., 2006; Guo et al., 2015;

229 Griffith et al., 2015; Guo et al., 2016). A similar strong reduction in $PM_{2.5}$ concentration and variations in aerosol composition

230 over the past several years were observed in different regions in China (Tao et al., 2017; Wang et al., 2020b; Ding et al., 2019a;

231 Wen et al., 2018). As a result of strong reductions in inorganic ion concentrations, ALWC decreased dramatically in 2018/2019

232 (14.8±20.4 μg m^{-3}), compared to that in 2015/2016 (24.4±27.0 μg m^{-3}). In short, anthropogenic pollutant emissions, as well

233 as aerosol concentration and composition varied significantly between 2015/2016 and 2018/2019 in Shanghai, which, as will

234 be discussed below, has important implications for the production of OS in ambient aerosols.

3.2 Molecular composition of sulfur-containing organic compounds

236 The organic compounds in ambient $PM_{2.5}$ identified using UPLC-ESI(-)-QToF-MS were classified into four groups based on

237 their elemental composition, i.e., CHO, CHON, CHOS, and CHONS. Figure 3a, b show the average mass spectra of organic

238 compounds in $PM_{2.5}$ over a typical winter (21-26 January 2019) and summer (23-28 July 2019) pollution episode. The S-

239 containing compounds were overall larger in molecular size than CHO and CHON compounds, likely because of the addition

240 of a sulfate group to the molecule. The molecular weight (MW) of most S-containing compounds was between 100-400 Da,

241 and a few between 400-700 Da. The high-MW CHOS species (400-700 Da, see Table S4) showed a larger contribution in

242 winter than in summer, suggesting that they are more likely to arise from anthropogenic sources than biogenic emissions.

243 Figure 3c shows the signal contribution of different compound categories as well as concentrations of sulfate, OM, and

244 quantified OS, and Fig. 3d, e shows the number of identified organic compounds in each category during two pollution

245 episodes. The CHOS compounds contributed most by signal and number to observed organic compounds in both winter and

246 summer. The signal contributions and number of unquantified CHOS and CHONS did not vary significantly from winter to

247 summer, whereas the signal contribution of quantified CHOS and CHONS species were significantly larger in summer than

248 in winter (on average 15% vs. 7% for CHOS and 11% vs. 7% for CHONS). As will be discussed later, the abundance of

249 quantified anthropogenic OS was fairly constant across different seasons, in striking contrast to biogenic OS that showed

250 strong seasonal variability. Therefore, lack of seasonal variability for unquantified CHOS and CHONS implies that they may

251 originate mainly from anthropogenic sources. In addition, both signal intensity and the number of CHO species increased

252 significantly in summer, compared to those in winter. In contrast, CHON compounds contributed substantially more to the

253 observed signals in winter than in summer (on average 25% vs. 7%), though their numbers are quite similar during the two

254 periods. This suggests an enhanced production and/or suppressed depletion of nitrogen-containing organic species in winter.

255 The CHOS compounds with an O/S ratio of ≥ 4 were assigned as potential OS species. Similarly, the CHONS compounds

256 with an O/(N+S) ratio of ≥ 7 could be assigned as potential NOS species (Lin et al., 2012a). The $C_8H_{17}O_4S^-$, $C_8H_{15}O_4S^-$, and

257 ~~$C_5H_{11}O_4S$, $C_{27}H_{53}O_{11}S^-$~~ were the highest OS peaks observed in the pollution episode in winter. The $C_8H_{17}O_4S^-$ and $C_8H_{15}O_4S^-$

258 species may be derived from the photooxidation of diesel fuel vapors according to previous chamber studies (Blair et al.,

259 2017). The $C_5H_{11}O_4S^-$ species was correlated well with $C_8H_{17}O_4S^-$ in 2015/2016 (r=0.76) and 2018/2019 (r=0.84), suggesting

260 it may also be derived from diesel fuel vapors. The highest NOS peak in winter is $C_{10}H_{16}NO_7S^-$, which likely originate from

261 monoterpene oxidation (Surratt et al., 2008). The $C_5H_{11}O_7S^-$, $C_{15}H_{29}O_5S^-$, and $C_{13}H_{25}O_5S^-$ were observed among the highest

262 OS peaks in the summer pollution episode. The $C_5H_{11}O_7S^-$ is an IEPOX-derived OS species (Surratt et al., 2010), while

263 $C_{15}H_{29}O_5S^-$ and $C_{13}H_{25}O_5S^-$ may be derived from the oxidation of diesel fuel vapors (Blair et al., 2017). The highest NOS

264 peak in summer is monoterpene-derived $C_{10}H_{16}NO_7S^-$, the same with that in winter.

265 **3.3 Quantified organosulfates**

266 In this study, we quantified twenty-nine OS and six NOS compounds using a variety of authentic and surrogate OS standards

267 (Table 1). The quantified OS and NOS accounted for 14-18% and 47-67% by intensity of identified CHOS and CHONS in

268 polluted winter days and 15-37% and 58-87%, in polluted summer days (Fig. 3c), respectively. ~~The quantified OS and NOS~~

269 ~~accounted for 14-18% and 47-67% by intensity of identified CHOS and CHONS, respectively, in polluted winter days and~~

270 ~~15-37% and 58-87%, respectively, in polluted summer days (Fig. 3c).~~ Increased contribution of the quantified OS and NOS

271 in summer is because they are mainly derived from biogenic VOCs, which have greater emissions in summer than in other

272 seasons (Guenther et al., 1995). We note that a large fraction of OS signals were not quantified owing to the lack of proper

273 standards in this study. As discussed above, these unquantified OS mainly originated from anthropogenic sources. Future

274 studies of their abundances and formation mechanisms are warranted.

275 Table 2 summarizes the seasonally and annually averaged concentrations of the quantified OS, as well as their contributions

276 to OM in 2015/2016 and 2018/2019. The average concentration of quantified OS was 65.5±77.5 ng m^{-3} in 2015/2016 and

277 59.4±79.7 ng m^{-3} in 2018/2019. Although there was little change in OS concentration in these two years, the contribution of

278 OS to OM was larger in 2018/2019 (0.66%±0.56%) than in 2015/2016 (0.57%±0.56%), mainly due to a significant reduction

279 of OM in 2018/2019. Since OS species are important tracers for SOA (Surratt et al., 2007b; Gomez-Gonzalez et al., 2008;

280 Surratt et al., 2008; McNeill et al., 2012; Zhang et al., 2012; Surratt et al., 2010; Lin et al., 2013), an increase of OS/OM ratios

281 in 2018/2019 implies an enhanced contribution of SOA to OA in Shanghai. A previous study by Ma et al. (2014) reported an

282 average OS concentration in urban Shanghai in 2012/2013 of about 8.6 ng m^{-3}, substantially smaller than the concentration

283 reported here. This is likely due to a different number of OS species quantified (17 vs. 35) and different OS standards used

284 (octyl and benzyl sulfates vs. seven authentic/surrogate standards) in Ma et al. (2014) and the present study. As can be seen

285 in Fig. 2e and Table 2, the OS concentration and OS/OM ratio both showed a strong seasonal variation and peaked in summer.

286 The concentration of OS and its contribution to OM in summertime Shanghai (on average, 114.1 ng m^{-3} and 1.13% in July

287 2015 and 102.1 ng m^{-3} and 1.18% in July 2019) were larger or comparable to those observed in Beijing (55.2 ng m^{-3}, 0.42%)

288 (Wang et al., 2018), ~~Centreville, AL (54.7 ng m^{-3}, 0.24%) (Hettiyadura et al., 2017),~~ and Birmingham, Alabama (205.4 ng m$^-$

289 ^{3}, 2% of OC) (Rattanavaraha et al., 2017), but significantly lower than those observed in Atlanta, GA (2366.4 ng m^{-3}, 16.5%

290 of OC) and Centreville, AL (812 ng m^{-3}, 7.3% of OC) (Hettiyadura et al., 2019) where the production of OS and SOA is

291 dominated by the oxidation of biogenic emissions. The contribution of OS to OM in wintertime Shanghai (on average, 0.32%

292 in January 2016 and 0.36% in January 2019) was larger than that observed in Xi'an (~0.2%) (Huang et al., 2018), though the

293 quantified OS concentrations in two regions were comparable. This may suggest a stronger secondary formation of OA in

294 Shanghai than in Xi'an, consistent with independent measurements by Huang et al. (2014).

295 To further characterize the seasonality and interannual variability of OS, as well as their origin and formation mechanisms,

296 the quantified OS were assigned to four different source categories based on their molecular composition and literature data

297 (Surratt et al., 2008; Surratt et al., 2007a; Nozière et al., 2010; Surratt et al., 2010; Schindelka et al., 2013; Zhang et al., 2014;

298 Riva et al., 2015; Riva et al., 2016b; Blair et al., 2017; Nestorowicz et al., 2018). The OS species for each OS source category

299 are listed in Table 1 and the seasonal and interannual variations in the abundance of grouped and individual OS are shown in

300 Fig. 4 and Table S5, respectively.

301 **3.3.1 Isoprene-derived organosulfates**

302 Isoprene-derived OS (hereafter referred to as OS_i) include ten C_{4-5} species and one dimeric species ($C_7H_9O_7S^-$). The average

303 concentration of OS_i in summer was 76.5±93.4 ng m^{-3} for 2015/2016 and 68.4±102.2 ng m^{-3} for 2018/2019, significantly

304 larger than the concentrations (10.4-17.1 ng m^{-3}) in other seasons (Fig. 4a). Similar strong seasonality of OS_i was also observed

305 in suburban areas in the Mid-Atlantic United States (Meade et al., 2016) and the Pearl River Delta in Southern China (He et

306 al., 2014) The significantly increased production of OS_i in summer is mainly a result of enhanced isoprene emissions

307 (Guenther et al., 1995) and photochemistry due to strong solar radiation and high temperatures in this warmer season.

308 The most abundant species among OS_i was 2-MT-OS ($C_5H_{11}O_7S^-$), produced by reactive uptake of IEPOX on sulfate during

309 the photooxidation of isoprene under low-NO$_x$ conditions (Surratt et al., 2010). The average concentration of 2-MT-OS was

310 ~31 ng m^{-3} in summer, contributing to about 45% of OS_i, whereas it decreased to 0.4-1.3 ng m^{-3} in other seasons, accounting

311 for only 4-10% of OS_i in 2015/2016 and 2018/2019 (see Table S5). In addition, 2-methylglyceric acid sulfate (2-MA-OS,

312 $C_4H_7O_7S^-$) was also abundantly detected with an average concentration of 4.5 ng m^{-3} in summer and 1.0-2.2 ng m^{-3} in other

313 seasons during the two sampling years. 2-MA-OS is formed from reactive uptake of methacrylic acid epoxide (MAE) (Lin et

314 al., 2013) and hydroxymethyl-methyl-lactone (HMML) (Nguyen et al., 2015) on sulfate aerosol during isoprene

315 photooxidation under high-NO$_x$ conditions. It is worthwhile noting that the concentration ratio of 2-MT-OS/2-MA-OS in

316 summer (6.8-7.8) is substantially larger than that in other seasons (0.31-0.78). This is consistent with a dramatic reduction of

317 NO$_x$ level (e.g., NO$_2$) in summer (~13 ppb) compared to that in other seasons (~24-34 ppb) (see Table S3S1). Furthermore,

318 the NO$_x$-influenced oxidation pathways may not be conducive to 2-MA-OS formation in summer, given that the formation of

319 reactive intermediates such as MAE is unfavorable at high temperatures owing to enhanced thermal decomposition of its

320 precursor methacryloylperoxynitrate (MPAN) (Worton et al., 2013). Since 2-MT-OS and 2-MA-OS are key tracers for

321 isoprene-derived SOA under low- and high-NO$_x$ conditions, respectively (Surratt et al., 2010; Lin et al., 2013; Nguyen et al.,

322 2015). The dramatically larger ratios of 2-MT-OS/2-MA-OS in summer than in other seasons therefore strongly suggests that

323 the low-NO$_x$ oxidation pathways dominated the production of isoprene-derived SOA in summer, while the processes favorable

324   under high-NO_x conditions were important SOA formation in other seasons. We note that the 2-MT-OS/2-MA-OS ratios

325   observed in summertime Shanghai are smaller than those (17.0-33.8) observed in less polluted environments such as the

326   southeastern United States (Hettiyadura et al., 2019; Budisulistiorini et al., 2015; Riva et al., 2019), but significantly larger

327   than those (0.55-1.57) observed in Beijing (Wang et al., 2018; Bryant et al., 2020) and the Pearl River Delta (PRD) region of

328   China (He et al., 2018).

329   Other abundant OS_i species include $C_5H_7O_7S^-$, $C_5H_9O_7S^-$, and $C_4H_7O_6S^-$. The $C_5H_7O_7S^-$ and $C_5H_9O_7S^-$ species can be produced

330   by photooxidation of isoprene (Surratt et al., 2008; Nestorowicz et al., 2018) and/or the oxidative aging of ~~methyltetrol~~

331   ~~sulfate~~2-MT-OS (Hettiyadura et al., 2015; Chen et al., 2020). The $C_4H_7O_6S^-$ can be generated both from sulfate radical reaction

332   with MACR/MVK (Nozière et al., 2010; Schindelka et al., 2013; Wach et al., 2019) and isoprene photooxidation (Lin et al.,

333   2013; Surratt et al., 2007a; Nestorowicz et al., 2018). The $C_5H_7O_7S^-$ and $C_4H_7O_6S^-$ are also consistent in molecular formula

334   with the OS species formed from the photooxidation of diesel fuel vapors (Blair et al., 2017). However, these two species had

335   moderate to strong correlations with MT-OS and $C_5H_9O_7S^-$ in different seasons expect for autumn ($C_5H_7O_7S^-$: r=0.68-0.96,

336     $C_4H_7O_6S^-$: r=0.62-0.96), indicating that they are mainly derived from isoprene oxidation. We note that the five most abundant

337   OS_i species as discussed above were moderately correlated with EC and CO in winter (r=0.5-0.67), suggesting that there

338   might be anthropogenic sources of isoprene in winter. Borbon et al. (2001) measured the hourly isoprene concentration at an

339   urban site in Lille, France for two years and found that isoprene was largely derived from vehicle emissions in winter. In

340   addition to OS species, two isoprene-derived NOSs ($C_5H_{10}NO_9S^-$ and $C_5H_8NO_{10}S^-$) were also observed, in particular in

341   summer.

342   **3.3.2 Monoterpene-derived organosulfates**

343   Monoterpene-derived OS (hereafter referred to as OS_m) include seven C_{7-10} OS species and three C_{9-10} NOS species. Compared

344   to the OS_i, the OS_m showed a weaker seasonal variation and a relatively larger abundance except in summer (Fig. 4b). This is

345   consistent with the fact that isoprene emissions have stronger seasonal variability than monoterpene emissions (Guenther et

346   al., 1995). The seasonally averaged concentrations of OS_m were higher in spring and summer, but lower in autumn and winter.

347   This is different from previous observations in 2012/2013 in Shanghai by Ma et al (2014). They found that the OS_m were

348   most abundant in summer, followed by autumn, winter, and spring. The differences in seasonal variations of OS_m observed

349   by the two studies may be attributed to different meteorological and chemical conditions that affected precursor emissions

350   and chemistry of OS_m formation over the sampling periods. Given that the OS_m concentration had an obvious daily variation,

351   the number of samples collected would significantly affect the seasonally averaged concentration. As such, the difference in

352   the number of samples collected each season (18-20 samples in this study versus 6 samples within three days in Ma et al.

353   (2014)) may also contribute to the different seasonality observed in two studies.

354   The NOS species such as $C_{10}H_{16}NO_7S^-$, $C_9H_{14}NO_8S^-$, and $C_{10}H_{16}NO_{10}S^-$ were the most abundant OS_m species, which arises

355   mainly from monoterpenes photooxidation in the presence of NO_x or nighttime NO_3 chemistry (Surratt et al., 2008; Iinuma

356   et al., 2007a). The concentrations of these three NOS were all lower in summer than in spring and autumn (Table S5),

357   consistent with the seasonal trend of NO_x concentrations (Fig. 2 and Table ~~S3~~S1). Similar seasonal variations for these NOS

358   species were also observed in the PRD region of China (He et al., 2014) and the Mid-Atlantic United States (Meade et al.,

359 2016). Among NOS species, the $C_{10}H_{16}NO_7S^-$ was most abundant, contributing to 22-48% of OS_m. This species had an annual

360 average concentration of 6.2 ± 6.5 ng m^{-3} in 2015/2016 and 5.5 ± 6.2 ng m^{-3} in 2018/2019, which is comparable to the

361 concentrations observed in Beijing (12 ng m^{-3}) (Wang et al., 2018) and Atlanta, GA (9.0 ng m^{-3}) (Hettiyadura et al., 2019),

362 but much lower than observed in the PRD region of China (52.4 ng m^{-3} in summer and 151 ng m^{-3} in autumn) (He et al.,

363 2014). The prevalence of monoterpene-derived NOS in Shanghai as observed in this study is consistent with recent

364 observations that monoterpenes accounted for up to 60% of nighttime NO_3 radical loss in the YRD region of China (Wang et

365 al., 2020a).

366 The most abundant nitrogen-free OS_m species was $C_{10}H_{15}O_7S^-$ (m/z 279.0538), which was shown to be produced from the

367 photooxidation of monoterpenes (Surratt et al., 2008) or sulfate radical reaction with α-pinene (Nozière et al., 2010). Although

368 the $C_{10}H_{15}O_7S^-$ is consistent in molecular composition with the OS species formed by photooxidation of cyclodecane in the

369 presence of sulfate aerosol (Riva et al., 2016b), its moderate to strong correlation (r=0.51-0.93) with the three monoterpene-

370 derived NOS in all seasons except for winter suggests that it is mainly derived from monoterpene oxidation. The concentration

371 of $C_{10}H_{15}O_7S^-$ was on average 3.0 ± 3.0 ng m^{-3} in 2015/2016, lower than that (4.0 ± 3.4 ng m^{-3}) in 2018/2019. In contrast to

372 NOS species, the $C_{10}H_{15}O_7S^-$ species was most abundant in summer in both years, again suggesting a strong contribution of

373 low-NO_x chemistry in OS and SOA formation in summer.

374 **3.3.3 Anthropogenic organosulfates**

375 The quantified anthropogenic OS (hereafter referred to as OS_a) in this study include phenyl sulfate ($C_6H_5O_4S^-$), benzyl sulfate

376 ($C_7H_7O_4S^-$), $C_8H_{17}O_4S^-$, as well as $C_4H_7O_4S^-$, $C_5H_7O_6S^-$, and $C_6H_9O_6S^-$. The annual average concentrations of OS_a in

377 2015/2016 and 2018/2019 were 5.6 ± 2.8 ng m^{-3} and 3.8 ± 3.3 ng m^{-3}, respectively. Although the concentration of quantified

378 OS_a decreased in 2018/2019, we are not sure whether the total concentration of OS_a decreased because only a small fraction

379 of OS_a were quantified. The inter-annual variations of OS_a warrants further studies. As shown in Fig. 4c, the quantified OS_a

380 concentration was substantially smaller compared to biogenic OS. In addition, the OS_a concentration had little seasonal

381 variations in both 2015/2016 and 2018/2019. Among quantified OS_a, the $C_4H_7O_4S^-$ was most abundant with an annual average

382 concentration of 2.0 ± 1.5 ng m^{-3} in 2015/2016 and 1.8 ± 2.6 ng m^{-3} in 2018/2019, which is comparable to the concentrations in

383 Atlanta,GA (Hettiyadura et al., 2019). Blair et al. (2017) found that photooxidation of diesel vapors in the presence of SO_2

384 can form $C_4H_7O_4S^-$, $C_5H_7O_6S^-$, and $C_6H_9O_6S^-$ species. The $C_8H_{17}O_4S^-$ species had the same retention time with the octyl

385 sulfate standard in the LC column, suggesting it is a long-chain aliphatic OS. This OS species was correlated with $C_5H_7O_6S^-$

386 and $C_6H_9O_6S^-$ that were potential diesel vapor-derived OS. Phenyl sulfate and benzyl sulfate may be produced by

387 photooxidation of naphthalene and 2-methylnaphthalene (Riva et al., 2015) and/or sulfate radical reaction with aromatic

388 compounds such as benzoic acid and toluene in the aqueous phase (Huang et al., 2020), but phenyl sulfate was only detected

389 in 42 out of 75 samples in 2015/2016 and 8 out of 81 samples in 2018/2019, primarily in winter. The benzyl sulfate

390 concentrations in 2015/2016 and 2018/2019 were 0.4 ± 0.1 ng m^{-3} and 0.2 ± 0.10 ng m^{-3}, respectively, which were higher than

391 the observations in springtime Lahore, Pakistan (Staudt et al., 2014) and in wintertime Xi'an, China (Huang et al., 2018).

392 Benzyl sulfate had a strong correlation with phenyl sulfate and was also correlated with $C_6H_9O_6S^-$ and $C_8H_{17}O_4S^-$.

393 **3.3.4 C_2/C_3 organosulfates**

The OS species with two or three carbon atoms are grouped together since many of them are considered to have both biogenic and anthropogenic origins. The C_2/C_3 OS quantified in this study include $C_2H_3O_6S^-$ (m/z 154.9650), $C_3H_5O_5S^-$ (m/z 152.9858), $C_3H_5O_6S^-$ (m/z 168.9807), $C_2H_3O_5S^-$ (m/z 138.9701), $C_3H_5O_4S^-$ (m/z 136.9909), and $C_3H_7O_5S^-$ (m/z 155.0014). The C_2/C_3 OS species averagely accounted for 19% of quantified OS concentrations and they were overall more abundant in summer than in other seasons in 2015/2016 and 2018/2019 (Fig. 4d). The $C_2H_3O_6S^-$, $C_3H_5O_5S^-$, and $C_3H_5O_6S^-$ species, which were previously assigned to glycolic acid sulfate (GAS), hydroxyacetone sulfate (HAS), and lactic acid sulfate (LAS), respectively (Olson et al., 2011; Hettiyadura et al., 2017; Huang et al., 2018; Wang et al., 2018; Hettiyadura et al., 2019), were among the most abundant C_2/C_3 OS species, together contributing to 76% of C_2/C_3 OS concentrations in 2015/2016 and 2018/2019. The concentration of $C_2H_3O_6S^-$ (GAS) was on average 2.9 ± 2.2 ng m^{-3} in 2015/2016 and 2.3 ± 1.7 ng m^{-3} in 2018/2019, which was lower than the concentrations measured in Beijing (19.5 ng m^{-3}) (Wang et al., 2018), Xi'an (77.3 ng m^{-3}) (Huang et al., 2018), Atlanta, GA (58.5 ng m^{-3}) (Hettiyadura et al., 2019), Centreville, AL (20.6 ng m^{-3}) (Hettiyadura et al., 2017), Lahore, Pakistan (11.3 ng m^{-3}), and Bakersfield, CA (4.5-5.4 ng m^{-3}) (Olson et al., 2011), and similar with those observed in Riverside, CA (3.3 ng m^{-3}) (Olson et al., 2011). We note that if accounting for the underestimation (2-6 times) in concentration due to matrix effects (see Sect. 2.5), the GAS concentration measured in Shanghai would be comparable to that in most of the regions mentioned above. The concentrations of $C_3H_5O_5S^-$ (HAS) and $C_3H_5O_6S^-$ (LAS) were quite similar, on average 2.3 and 2.2 ng m^{-3} in 2015/2016 and 1.8 and 1.9 ng m^{-3} in 2018/2019, respectively, which were comparable to the concentrations observed in Beijing (2.2 ng m^{-3} and 4.4 ng m^{-3}) (Wang et al., 2018), and Xi'an (1.3 ng m^{-3} for HAS) (Huang et al., 2018), but lower than those measured in Centreville, AL (5.8 ng m^{-3} and 16.5 ng m^{-3}) (Hettiyadura et al., 2017) and Atlanta, GA (10.1 ng m^{-3} and 38.4 ng m^{-3}) (Hettiyadura et al., 2019). The $C_2H_3O_6S^-$, $C_3H_5O_5S^-$, $C_3H_5O_6S^-$, and $C_2H_3O_5S^-$ were strongly correlated with most of OS_i OS_i species (r=0.52-0.96 for $C_2H_3O_6S^-$, r=0.53-0.99 for $C_3H_5O_5S^-$, r=0.53-0.90 for $C_3H_5O_6S^-$, and r=0.53-0.94 for $C_2H_3O_5S^-$), indicating that they originated mainly from isoprene chemistry. This is in line with recent findings that a series of C_2/C_3 OS species, including $C_2H_3O_6S^-$, $C_3H_5O_6S^-$, and $C_2H_3O_5S^-$, can be produced by heterogeneous OH oxidation of particulate 2-MT-OS (Chen et al., 2020). The $C_3H_5O_4S^-$ species, proposed to contain an allyl group (Hettiyadura et al., 2017), was previously found to be produced by diesel photooxidation (Blair et al., 2017), and was correlated with anthropogenic OS such as the potential diesel vapor-derived OS ($C_8H_{17}O_4S^-$, $C_4H_7O_4S^-$, $C_5H_7O_6S^-$, and $C_6H_9O_6S^-$, r=0.53-0.87) and benzyl sulfate ($C_7H_7O_4S^-$, r=0.49-0.88). The $C_3H_7O_5S^-$ is likely an OS species containing one hydroxyl group (Hettiyadura et al., 2017), which was strongly correlated with the $C_3H_5O_4S^-$ in all seasons and correlated with the diesel vapor-derived OS_a ($C_6H_9O_6S^-$ and $C_8H_{17}O_4S^-$) in spring and autumn, suggesting that it may be largely derived from the photooxidation of diesel vapors. This result is different from the observations in Atlanta, GA, where the $C_3H_7O_5S^-$ was correlated with most of OS_i, leading to the suggestion that it was derived from the oxidation of isoprene (Hettiyadura et al., 2019). We note that the concentrations of $C_3H_5O_4S^-$ and $C_3H_7O_5S^-$ species decreased significantly from 2015/2016 to 2018/2019 (except for summer, see Table S5), overall consistent with the interannual variations of OS_a species. This further supports that these two OS species mainly originated from anthropogenic sources.

3.4 Factors influencing organosulfate formation

Laboratory and field studies have shown that aerosol properties such as acidity, sulfate concentration, and ALWC play important roles in the formation of OS (Iinuma et al., 2007b; Chan et al., 2011; Surratt et al., 2007a; Surratt et al., 2007b; Liao

et al., 2015; Hettiyadura et al., 2019; Riva et al., 2019). Here we examined the influences of these factors, as well as the level of oxidants and temperature on OS formation in ambient aerosols in Shanghai. Aerosol pH and ALWC here were calculated using ISORROPIA-II (see Sect. 2.4). Figure 5 shows the OS concentration versus the O_x level, sulfate concentration, aerosol pH, and ALWC observed in the spring, autumn, and winter of 2015-2016 and 2018-2019. Since the OS concentrations in summer were significantly greater than in other seasons, they were plotted separately in Fig. 6. As shown in Figs. 5 and 6, the aerosol pH in Shanghai ranged between 1.5 and 5.3 in summer and between 2.5 and 6.1 in other seasons, overall within the pH range (2-6) reported for ambient aerosols in northern China (Liu et al., 2017; Shi et al., 2017; Ding et al., 2019b; Song et al., 2019; Wang et al., 2018). A recent study by Zheng et al. (2020) has suggested that aerosol pH levels in populated continental regions including eastern and northern China are widely buffered by ammonium/ammonia, where the variation in aerosol pH is mainly driven by the variation in ALWC and temperature. Therefore, we infer that the lower aerosol pH in summer than in other seasons in Shanghai was mainly a result of decreased ALWC (Figs. 5 and 6c, d) and enhanced temperature (Fig. 2a). Decreased aerosol pH in summer compared to other seasons were also observed in Beijing (Ding et al., 2019b) and the southeastern United States (Guo et al., 2015; Nah et al., 2018).

As can be seen in Fig. 5, the OS concentration in spring, autumn, and winter increased obviously with increasing O_x level, sulfate concentration, and aerosol acidity (Fig. 5a, b). A similar result was also found in Beijing that most OS species were correlated strongly with the product of ozone and particulate sulfate ($[O_3]\cdot[SO_4^{2-}]$) (Bryant et al., 2020). In addition, an overall positive correlation was observed between the OS concentration and ALWC (Fig. 5c, d). Therefore, it is likely that that the OS species were mainly produced by acid-catalyzed heterogeneous/aqueous-phase reactions of oxidized organic compounds with sulfate in these seasons. Previous studies have shown that elevated ALWC could inhibit OS production by decreasing aerosol acidity through dilution (Lewandowski et al., 2015; Nestorowicz et al., 2018). However, as the increase of ALWC was accompanied by elevated sulfate concentration, such a decrease in aerosol acidity was not observed in the present study (Fig. 5c, d). Alternatively, the increased ALWC likely promoted the mass transfer of oxidized organics into the aerosol phase, thereby enhancing OS formation. We note that the observations with moderate to high ALWC but relatively low OS concentration (data points in the triangle in Fig. 5c, d) were associated with low O_x levels (<50 ppb) that significantly limited the oxidation of VOC precursors and hence the formation of OS.

As seen in Fig. 6, OS production in summer increased dramatically with rising O_x concentration. In addition, high OS concentrations were associated with high ambient temperatures, which can enhance emissions of biogenic precursors and the production of O_x. While the aerosol acidity effect on OS production in summer was still evident, the influence of sulfate and ALWC was not as obvious as in other seasons. This is likely because the OS production in summer was driven by the strong emission and fast photochemistry of VOC precursors. It is noteworthy that the sulfate concentrations, ALWC, and aerosol acidities were overall higher in 2015/2016 than in 2018/2019, but the OS concentrations were similar in two years. This implies that the O_x level is a driving factor for OS formation in ambient aerosols in Shanghai. Very recently, a similar oxidant effect on OS formation was also observed in urban Beijing (Bryant et al., 2020). Therefore, mitigation of O_x pollution may effectively reduce the production of OS and SOA in Chinese megacities.

4 Conclusions

In this study, we collected ambient $PM_{2.5}$ filter samples over four seasons in 2015/2016 and 2018/2019 in urban Shanghai, China, and comprehensively characterized the sulfur-containing organic compounds (CHOS and CHONS) in these $PM_{2.5}$ samples using UPLC-ESI(-)-QToF-MS. The CHOS and CHONS species accounted for a large fraction of ion signals for organic compounds in ambient $PM_{2.5}$. Using a set of authentic and surrogate OS standards, we quantified the abundance of 29 OS and 6 NOS species in ambient aerosols. We find that there was no strong change in the OS concentration in 2018/2019 (59.4±79.7 ng m^{-3}) compared to that in 2015/2016 (65.5±77.5 ng m^{-3}), though the OM concentration decreased by 29% between 2015/2016 (12.7±8 μg m^{-3}) and 2018/2019 (9±5.5 μg m^{-3}). As a result, the annual average contribution of quantified OS to OM increased from 0.57% in 2015/2016 to 0.66% in 2018/2019, suggesting an enhanced contribution of SOA to OM in Shanghai in recent years. Isoprene- and monoterpene-derived organosulfates (OS_i and OS_m) accounted for 36.3% and 31.0% of the quantified OS concentrations, respectively, during the two sampling years, indicating a significant contribution of biogenic emissions to SOA in Shanghai. The abundance of OS_i had strong seasonality and was significantly higher in summer (76.5±93.4 ng m^{-3} in 2015/2016 and 68.4±102.2 ng m^{-3} in 2018/2019) than in other seasons (10.4-17.1 ng m^{-3}). The OS_m concentration showed a weaker seasonal variation and was relatively higher in spring and summer than in autumn and winter. In contrast, anthropogenic OS (OS_a) had little seasonal variations and decreased by 32% from 2015/2016 to 2018/2019. The C_2/C_3 OS species that were more abundant in summer than in other seasons, on average contributed to 19% of the concentration of quantified OS species. The $C_2H_3O_6S^-$ (GAS), $C_3H_5O_5S^-$ (HAS), and $C_3H_5O_6S^-$ (LAS), which were derived mainly from isoprene chemistry, were the most abundant C_2/C_3 OS species and together accounted for 76% of C_2/C_3 OS concentrations.

2-MT-OS was the most abundant OS species in summer. The dramatic larger 2-MT-OS/2-MA-OS ratios in summer (6.8-7.8) versus other seasons (0.31-0.78) implies that the reaction pathways prevalent under low-NO_x conditions (e.g., reactive uptake of IEPOX and photooxidation of ISOPOOH) dominated the production of OS_i and isoprene-derived SOA in summer, while the processes favorable under high-NO_x conditions play an important role in OS_i and SOA formation in other seasons. The $C_{10}H_{16}NO_7S^-$ species derived from monoterpenes was the most abundant NOS species, with an annual average concentration of 6.2±6.5 ng m^{-3} in 2015/2016 and 5.5±6.2 ng m^{-3} in 2018/2019. This agrees well with previous observations that monoterpenes depleted about 60% of nighttime NO_3 radicals in the YRD region of China (Wang et al., 2020a).

In addition, we find that the abundance of OS is overall positively correlated with the O_x level, sulfate concentration, aerosol acidity, as well as ALWC in spring, autumn, and winter, suggesting the production of OS via acid-catalyzed aqueous-phase reactions of oxidized organic compounds on sulfate. However, OS production in summer was strongly driven by rising O_x and temperature that could enhance the photochemistry and emissions of biogenic precursors. We further find that although sulfate concentrations, aerosol acidities, and ALWC were significantly lower in 2018/2019 than in 2015/2016, the production of OS was largely sustained in 2018/2019 by the nearly unchanged O_x level that maintained the fast oxidation of VOC precursors. These results imply that controlling O_x pollution may also effectively mitigate particulate organic matter pollution in eastern China.

It should be pointed out that GAS was likely underestimated by a factor of 2-6 as a result of the matrix effect during the analysis in our study. If accounting for this effect, it would be the second most abundant OS species after MT-OS. In addition,

a large fraction of CHOS signals that arose mainly from anthropogenic sources were not quantified due to the lack of proper OS standards in this study. Therefore, the OS concentration and its contribution to organic aerosol in Shanghai could be significantly greater. Future studies on the abundance, origin, and formation mechanisms of these unquantified OS are warranted for a better understanding of the formation and evolution of OS and SOA in the atmosphere.

Data availability. The data presented in this work are available upon request from the corresponding author (yuezhao20@sjtu.edu.cn).

Author contributions. YZ designed and led the research, YW, WFZ, and ZC collected ambient samples, YCW and JZY provided OS standards, JYS conducted ISORROPIA-II model calculation, YW conducted sample analysis, and YZ and YW processed the data and wrote the paper with contributions from all of the authors.

Competing interests. The authors declare no conflict of interest.

Acknowledgments. This work was supported by the National Natural Science Foundation of China (Grant 21806104), the Science and Technology Commission of Shanghai Municipality (Grant 19DZ1205004), and the Program for Professor of Special Appointment (Eastern Scholar) at Shanghai Institutions of Higher Learning.

References

Behera, S. N., Cheng, J., Huang, X., Zhu, Q., Liu, P., and Balasubramanian, R.: Chemical composition and acidity of size-fractionated inorganic aerosols of 2013-14 winter haze in Shanghai and associated health risk of toxic elements, Atmos. Environ., 122, 259-271, 10.1016/j.atmosenv.2015.09.053, 2015.

Blair, S. L., MacMillan, A. C., Drozd, G. T., Goldstein, A. H., Chu, R. K., Pasa-Tolic, L., Tolic, N., Lin, P., Laskin, J., Laskin, A., and Nizkorodov, S. A.: Molecular Characterization of Organosulfur Compounds in Biodiesel and Diesel Fuel Secondary Organic Aerosol, Environ. Sci. Technol., 51, 119-127, 10.1021/acs.est.6b03304, 2017.

Borbon, A., Fontaine, H., Veillerot, M., Locoge, N., Galloo, J. C., and Guillermo, R.: An investigation into the traffic-related fraction of isoprene at an urban location, Atmos. Environ., 35, 3749-3760, 2001.

Brüggemann, M., Poulain, L., Held, A., Stelzer, T., Zuth, C., Richters, S., Mutzel, A., van Pinxteren, D., Iinuma, Y., Katkevica, S., Rabe, R., Herrmann, H., and Hoffmann, T.: Real-time detection of highly oxidized organosulfates and BSOA marker compounds during the F-BEACh 2014 field study, Atmos. Chem. Phys., 17, 1453-1469, 10.5194/acp-17-1453-2017, 2017.

Brüggemann, M., Xu, R. S., Tilgner, A., Kwong, K. C., Mutzel, A., Poon, H. Y., Otto, T., Schaefer, T., Poulain, L., Chan, M. N., and Herrmann, H.: Organosulfates in ambient aerosol: state of knowledge and future research directions on formation, abundance, fate, and importance, Environ. Sci. Technol., 54, 3767-3782, doi: 10.1021/acs.est.9b06751, 2020.

Bryant, D. J., Dixon, W. J., Hopkins, J. R., Dunmore, R. E., Pereira, K. L., Shaw, M., Squires, F. A., Bannan, T. J., Mehra, A., Worrall, S. D., Bacak, A., Coe, H., Percival, C. J., Whalley, L. K., Heard, D. E., Slater, E. J., Ouyang, B., Cui, T., Surratt, J. D., Liu, D., Shi, Z., Harrison, R., Sun, Y., Xu, W., Lewis, A. C., Lee, J. D., Rickard, A. R., and Hamilton, J. F.: Strong anthropogenic control of secondary organic aerosol formation from isoprene in Beijing, Atmos. Chem. Phys., 20, 7531-7552, 10.5194/acp-20-7531-2020, 2020.

Budisulistiorini, S. H., Li, X., Bairai, S. T., Renfro, J., Liu, Y., Liu, Y. J., McKinney, K. A., Martin, S. T., McNeill, V. F., Pye, H. O. T., Nenes, A., Neff, M. E., Stone, E. A., Mueller, S., Knote, C., Shaw, S. L., Zhang, Z., Gold, A., and Surratt, J. D.: Examining the effects of anthropogenic emissions on isoprene-derived secondary organic aerosol formation during the 2013 Southern Oxidant and Aerosol Study (SOAS) at the Look Rock, Tennessee ground site, Atmos. Chem. Phys., 15, 8871-8888, 10.5194/acp-15-8871-2015, 2015.

Chan, M. N., Surratt, J. D., Claeys, M., Edgerton, E. S., Tanner, R. L., Shaw, S. L., Zheng, M., Knipping, E. M., Eddingsaas, N. C., Wennberg, P. O., and Seinfeld, J. H.: Characterization and quantification of isoprene-derived epoxydiols in ambient aerosol in the southeastern United States, Environ. Sci. Technol., 44, 4590-4596, 10.1021/es100596b, 2010.

Chan, M. N., Surratt, J. D., Chan, A. W. H., Schilling, K., Offenberg, J. H., Lewandowski, M., Edney, E. O., Kleindienst, T. E., Jaoui, M., Edgerton, E. S., Tanner, R. L., Shaw, S. L., Zheng, M., Knipping, E. M., and Seinfeld, J. H.: Influence of aerosol acidity on the chemical composition of secondary organic aerosol from beta-caryophyllene, Atmos. Chem. Phys., 11, 1735-1751, 10.5194/acp-11-1735-2011, 2011.

Chen, Y., Zhang, Y., Lambe, A. T., Xu, R., Lei, Z., Olson, N. E., Zhang, Z., Szalkowski, T., Cui, T., Vizuete, W., Gold, A., Turpin, B. J., Ault, A. P., Chan, M. N., and Surratt, J. D.: Heterogeneous hydroxyl radical oxidation of isoprene-epoxydiol-derived

548 methyltetrol sulfates: plausible formation mechanisms of previously unexplained organosulfates in ambient fine aerosols,
549 Environ. Sci. Technol. Lett., 7, 460-468, 10.1021/acs.estlett.0c00276, 2020.

550 Claeys, M., Wang, W., Vermeylen, R., Kourtchev, I., Chi, X., Farhat, Y., Surratt, J. D., Gomez-Gonzalez, Y., Sciare, J., and Maenhaut,
551 W.: Chemical characterisation of marine aerosol at Amsterdam Island during the austral summer of 2006-2007, J. Aerosol Sci.,
552 41, 13-22, 10.1016/j.jaerosci.2009.08.003, 2010.

553 Darer, A. I., Cole-Filipiak, N. C., O'Connor, A. E., and Elrod, M. J.: Formation and stability of atmospherically relevant isoprene-
554 derived organosulfates and organonitrates, Environ. Sci. Technol., 45, 1895-1902, 10.1021/es103797z, 2011.

555 DeRieux, W.-S., Li, Y., Lin, P., Laskin, J., Laskin, A., Bertram, A. K., Nizkorodov, S. A., and Shiraiwa, M.: Predicting the glass
556 transition temperature and viscosity of secondary organic material using molecular composition, Atmos. Chem. Phys., 18, 6331-
557 6351, 10.5194/acp-18-6331-2018, 2018.

558 Ding, A., Huang, X., Nie, W., Chi, X., Xu, Z., Zheng, L., Xu, Z., Xie, Y., Qi, X., Shen, Y., Sun, P., Wang, J., Wang, L., Sun, J., Yang,
559 X.-Q., Qin, W., Zhang, X., Cheng, W., Liu, W., Pan, L., and Fu, C.: Significant reduction of PM2.5 in eastern China due to
560 regional-scale emission control: evidence from SORPES in 2011-2018, Atmos. Chem. Phys., 19, 11791-11801, 10.5194/acp-
561 19-11791-2019, 2019a.

562 Ding, J., Zhao, P. S., Su, J., Dong, Q., Du, X., and Zhang, Y. F.: Aerosol pH and its driving factors in Beijing, Atmos. Chem. Phys.,
563 19, 7939-7954, 10.5194/acp-19-7939-2019, 2019b.

564 Estillore, A. D., Hettiyadura, A. P. S., Qin, Z., Leckrone, E., Wombacher, B., Humphry, T., Stone, E. A., and Grassian, V. H.: Water
565 uptake and hygroscopic growth of organosulfate aerosol, Environ. Sci. Technol., 50, 4259-4268, 10.1021/acs.est.5b05014, 2016.

566 Fisseha, R., Dommen, J., Gutzwiller, L., Weingartner, E., Gysel, M., Emmenegger, C., Kalberer, M., and Baltensperger, U.: Seasonal
567 and diurnal characteristics of water soluble inorganic compounds in the gas and aerosol phase in the Zurich area, Atmos. Chem.
568 Phys., 6, 1895-1904, 10.5194/acp-6-1895-2006, 2006.

569 Fleming, L. T., Ali, N. N., Blair, S. L., Roveretto, M., George, C., and Nizkorodov, S. A.: Formation of light-absorbing
570 organosulfates during evaporation of secondary organic material extracts in the presence of sulfuric acid, ACS Earth Space
571 Chem., 3, 947-957, 10.1021/acsearthspacechem.9b00036, 2019.

572 Fountoukis, C. and Nenes, A.: ISORROPIA II: a computationally efficient thermodynamic equilibrium model for K^+-Ca^{2+}-Mg^{2+}-
573 NH_4^+-Na^+-SO_4^{2-}-NO_3^--Cl^--H_2O aerosols, Atmos. Chem. Phys., 7, 4639-4659, 10.5194/acp-7-4639-2007, 2007.

574 Froyd, K. D., Murphy, S. M., Murphy, D. M., de Gouw, J. A., Eddingsaas, N. C., and Wennberg, P. O.: Contribution of isoprene-
575 derived organosulfates to free tropospheric aerosol mass, P. Natl. Acad. Sci. USA, 107, 21360-21365, 10.1073/pnas.1012561107,
576 2010.

577 Gómez-González, Y., Surratt, J. D., Cuyckens, F., Szmigielski, R., Vermeylen, R., Jaoui, M., Lewandowski, M., Offenberg, J. H.,
578 Kleindienst, T. E., Edney, E. O., Blockhuys, F., Van Alsenoy, C., Maenhaut, W., and Claeys, M.: Characterization of
579 organosulfates from the photooxidation of isoprene and unsaturated fatty acids in ambient aerosol using liquid
580 chromatography/(-) electrospray ionization mass spectrometry, J. Mass Spectrom., 43, 371-382, 10.1002/jms.1329, 2008.

581 Grgic, I., Dovzan, A., Bercic, G., and Hudnik, V.: The effect of atmospheric organic compounds on the Fe-catalyzed S(IV)
582 autoxidation in aqueous solution, J. Atmos. Chem., 29, 315-337, 10.1023/a:1005918912994, 1998.

583 Griffith, S. M., Huang, X. H. H., Louie, P. K. K., and Yu, J. Z.: Characterizing the thermodynamic and chemical composition factors
584 controlling PM2.5 nitrate: Insights gained from two years of online measurements in Hong Kong, Atmos. Environ., 122, 864-
585 875, 10.1016/j.atmosenv.2015.02.009, 2015.

586 Guenther, A., Hewitt, C. N., Erickson, D., Fall, R., Geron, C., Graedel, T., Harley, P., Klinger, L., Lerdau, M., McKay, W. A., Pierce,
587 T., Scholes, B., Steinbrecher, R., Tallamraju, R., Taylor, J., and Zimmerman, P.: A global model of natural volatile organic
588 compound emissions, J. Geophys. Res., 100, 8873-8892, doi: 10.1029/94JD02950, 1995.

589 Guo, H., Xu, L., Bougiatioti, A., Cerully, K. M., Capps, S. L., Hite, J. R., Carlton, A. G., Lee, S. H., Bergin, M. H., Ng, N. L., Nenes,
590 A., and Weber, R. J.: Fine-particle water and pH in the southeastern United States, Atmos. Chem. Phys., 15, 5211-5228,
591 10.5194/acp-15-5211-2015, 2015.

592 Guo, H., Sullivan, A. P., Campuzano-Jost, P., Schroder, J. C., Lopez-Hilfiker, F. D., Dibb, J. E., Jimenez, J. L., Thornton, J. A.,
593 Brown, S. S., Nenes, A., and Weber, R. J.: Fine particle pH and the partitioning of nitric acid during winter in the northeastern
594 United States, J. Geophys. Res. Atmos., 121, 10355-10376, 10.1002/2016jd025311, 2016.

595 Hansen, A. M. K., Kristensen, K., Nguyen, Q. T., Zare, A., Cozzi, F., Nøjgaard, J. K., Skov, H., Brandt, J., Christensen, J. H., Ström,
596 J., Tunved, P., Krejci, R., and Glasius, M.: Organosulfates and organic acids in Arctic aerosols: speciation, annual variation and
597 concentration levels, Atmos. Chem. Phys., 14, 7807-7823, 10.5194/acp-14-7807-2014, 2014.

598 Hansen, A. M. K., Hong, J., Raatikainen, T., Kristensen, K., Ylisirnio, A., Virtanen, A., Petaja, T., Glasius, M., and Prisle, N. L.:
599 Hygroscopic properties and cloud condensation nuclei activation of limonene-derived organosulfates and their mixtures with
600 ammonium sulfate, Atmos. Chem. Phys., 15, 14071-14089, 10.5194/acp-15-14071-2015, 2015.

601 Hatch, L. E., Creamean, J. M., Ault, A. P., Surratt, J. D., Chan, M. N., Seinfeld, J. H., Edgerton, E. S., Su, Y., and Prather, K. A.:
602 Measurements of isoprene-derived organosulfates in ambient aerosols by aerosol time-of-flight mass spectrometry-part 2:
603 temporal variability and formation mechanisms, Environ. Sci. Technol., 45, 8648-8655, 10.1021/es2011836, 2011.

604 Hawkins, L. N., Russell, L. M., Covert, D. S., Quinn, P. K., and Bates, T. S.: Carboxylic acids, sulfates, and organosulfates in
605 processed continental organic aerosol over the southeast Pacific Ocean during VOCALS-REx 2008, J. Geophys. Res., 115,
606 10.1029/2009jd013276, 2010.

607 He, Q. F., Ding, X., Wang, X. M., Yu, J. Z., Fu, X. X., Liu, T. Y., Zhang, Z., Xue, J., Chen, D. H., Zhong, L. J., and Donahue, N. M.:
608 Organosulfates from pinene and isoprene over the Pearl River Delta, South China: seasonal variation and implication in
609 formation mechanisms, Environ. Sci. Technol., 48, 9236-9245, 10.1021/es501299v, 2014.

610 He, Q. F., Ding, X., Fu, X. X., Zhang, Y. Q., Wang, J. Q., Liu, Y. X., Tang, M. J., Wang, X. M., and Rudich, Y.: Secondary organic
611   aerosol formation from isoprene epoxides in the Pearl River Delta, South China: IEPOX- and HMML-derived tracers, J.
612   Geophys. Res.-Atmos., 123, 6999-7012, 10.1029/2017jd028242, 2018.
613 Hennigan, C. J., Izumi, J., Sullivan, A. P., Weber, R. J., and Nenes, A.: A critical evaluation of proxy methods used to estimate the
614   acidity of atmospheric particles, Atmos. Chem. Phys., 15, 2775-2790, 10.5194/acp-15-2775-2015, 2015.
615 Herrmann, H.: Kinetics of aqueous phase reactions relevant for atmospheric chemistry, Chem. Rev., 103, 4691-4716,
616   10.1021/cr020658q, 2003.
617 Hettiyadura, A. P. S., Stone, E. A., Kundu, S., Baker, Z., Geddes, E., Richards, K., and Humphry, T.: Determination of atmospheric
618   organosulfates using HILIC chromatography with MS detection, Atmos. Meas. Tech., 8, 2347-2358, 10.5194/amt-8-2347-2015,
619   2015.
620 Hettiyadura, A. P. S., Jayarathne, T., Baumann, K., Goldstein, A. H., de Gouw, J. A., Koss, A., Keutsch, F. N., Skog, K., and Stone,
621   E. A.: Qualitative and quantitative analysis of atmospheric organosulfates in Centreville, Alabama, Atmos. Chem. Phys., 17,
622   1343-1359, 10.5194/acp-17-1343-2017, 2017.
623 Hettiyadura, A. P. S., Al-Naiema, I. M., Hughes, D. D., Fang, T., and Stone, E. A.: Organosulfates in Atlanta, Georgia: anthropogenic
624   influences on biogenic secondary organic aerosol formation, Atmos. Chem. Phys., 19, 3191-3206, 10.5194/acp-19-3191-2019,
625   2019.
626 Hoffmann, T., Huang, R. J., and Kalberer, M.: Atmospheric analytical chemistry, Anal. Chem., 83, 4649-4664, 10.1021/ac2010718,
627   2011.
628 Huang, L., Coddens, E. M., and Grassian, V. H.: Formation of organosulfur compounds from aqueous phase reactions of S(IV) with
629   methacrolein and methyl vinyl ketone in the presence of transition metal ions, ACS Earth Space Chem., 3, 1749-1755,
630   10.1021/acsearthspacechem.9b00173, 2019.
631 Huang, L., Liu, T., and Grassian, V. H.: Radical-initiated formation of aromatic organosulfates and sulfonates in the aqueous phase,
632   Environ. Sci. Technol., 54, 11857-11864, 10.1021/acs.est.0c05644, 2020.
633 Huang, R.-J., Zhang, Y., Bozzetti, C., Ho, K.-F., Cao, J.-J., Han, Y., Daellenbach, K. R., Slowik, J. G., Platt, S. M., Canonaco, F.,
634   Zotter, P., Wolf, R., Pieber, S. M., Bruns, E. A., Crippa, M., Ciarelli, G., Piazzalunga, A., Schwikowski, M., Abbaszade, G.,
635   Schnelle-Kreis, J., Zimmermann, R., An, Z., Szidat, S., Baltensperger, U., El Haddad, I., and Prevot, A. S. H.: High secondary
636   aerosol contribution to particulate pollution during haze events in China, Nature, 514, 218-222, 10.1038/nature13774, 2014.
637 Huang, R.-J., Cao, J., Chen, Y., Yang, L., Shen, J., You, Q., Wang, K., Lin, C., Xu, W., Gao, B., Li, Y., Chen, Q., Hoffmann, T., amp,
638   apos, Dowd, C. D., Bilde, M., and Glasius, M.: Organosulfates in atmospheric aerosol: synthesis and quantitative analysis of
639   PM$_{2.5}$ from Xi'an, northwestern China, Atmos. Meas. Tech., 11, 3447-3456, 10.5194/amt-11-3447-2018, 2018.
640 Iinuma, Y., Mueller, C., Berndt, T., Boege, O., Claeys, M., and Herrmann, H.: Evidence for the existence of organosulfates from β-
641   pinene ozonolysis in ambient secondary organic aerosol, Environ. Sci. Technol., 41, 6678-6683, 2007a.
642 Iinuma, Y., Mueller, C., Boege, O., Gnauk, T., and Herrmann, H.: The formation of organic sulfate esters in the limonene ozonolysis
643   secondary organic aerosol (SOA) under acidic conditions, Atmos. Environ., 41, 5571-5583, 10.1016/j.atmosenv.2007.03.007,
644   2007b.
645 Iinuma, Y., Boege, O., Kahnt, A., and Herrmann, H.: Laboratory chamber studies on the formation of organosulfates from reactive
646   uptake of monoterpene oxides, Phys. Chem. Chem. Phys., 11, 7985-7997, 10.1039/b904025k, 2009.
647 Jiang, P.-Y., Katsumura, Y., Domae, M., Ishikawa, K., Ishigure, K., and Yoshida, Y.: Pulse radiolysis study of concentrated sulfuric
648   acid solutions. Formation mechanism, yield and reactivity of sulfate radicals, J. Chem. Soc., Faraday Trans., 88,
649   10.1039/ft9928801653, 1992.
650 Jimenez, J. L., Canagaratna, M. R., Donahue, N. M., Prevot, A. S. H., Zhang, Q., Kroll, J. H., DeCarlo, P. F., Allan, J. D., Coe, H.,
651   Ng, N. L., Aiken, A. C., Docherty, K. S., Ulbrich, I. M., Grieshop, A. P., Robinson, A. L., Duplissy, J., Smith, J. D., Wilson, K.
652   R., Lanz, V. A., Hueglin, C., Sun, Y. L., Tian, J., Laaksonen, A., Raatikainen, T., Rautiainen, J., Vaattovaara, P., Ehn, M., Kulmala,
653   M., Tomlinson, J. M., Collins, D. R., Cubison, M. J., Dunlea, E. J., Huffman, J. A., Onasch, T. B., Alfarra, M. R., Williams, P.
654   I., Bower, K., Kondo, Y., Schneider, J., Drewnick, F., Borrmann, S., Weimer, S., Demerjian, K., Salcedo, D., Cottrell, L., Griffin,
655   R., Takami, A., Miyoshi, T., Hatakeyama, S., Shimono, A., Sun, J. Y., Zhang, Y. M., Dzepina, K., Kimmel, J. R., Sueper, D.,
656   Jayne, J. T., Herndon, S. C., Trimborn, A. M., Williams, L. R., Wood, E. C., Middlebrook, A. M., Kolb, C. E., Baltensperger, U.,
657   and Worsnop, D. R.: Evolution of Organic Aerosols in the Atmosphere, Science, 326, 1525-1529, 10.1126/science.1180353,
658   2009.
659 Johnston, M. V. and Kerecman, D. E.: Molecular characterization of atmospheric organic aerosol by mass spectrometry, Annu. Rev.
660   Anal. Chem., 12, 247-274, 10.1146/annurev-anchem-061516-045135, 2019.
661 Kourtchev, I., Godoi, R. H. M., Connors, S., Levine, J. G., Archibald, A. T., Godoi, A. F. L., Paralovo, S. L., Barbosa, C. G. G.,
662   Souza, R. A. F., Manzi, A. O., Seco, R., Sjostedt, S., Park, J.-H., Guenther, A., Kim, S., Smith, J., Martin, S. T., and Kalberer,
663   M.: Molecular composition of organic aerosols in central Amazonia: an ultra-high-resolution mass spectrometry study, Atmos.
664   Chem. Phys., 16, 11899-11913, 10.5194/acp-16-11899-2016, 2016.
665 Kristensen, K. and Glasius, M.: Organosulfates and oxidation products from biogenic hydrocarbons in fine aerosols from a forest
666   in North West Europe during spring, Atmos. Environ., 45, 4546-4556, 10.1016/j.atmosenv.2011.05.063, 2011.
667 Kundu, S., Quraishi, T. A., Yu, G., Suarez, C., Keutsch, F. N., and Stone, E. A.: Evidence and quantitation of aromatic organosulfates
668   in ambient aerosols in Lahore, Pakistan, Atmos. Chem. Phys., 13, 4865-4875, 10.5194/acp-13-4865-2013, 2013.
669 Le Breton, M., Wang, Y., Hallquist, Å. M., Pathak, R. K., Zheng, J., Yang, Y., Shang, D., Glasius, M., Bannan, T. J., Liu, Q., Chan,
670   C. K., Percival, C. J., Zhu, W., Lou, S., Topping, D., Wang, Y., Yu, J., Lu, K., Guo, S., Hu, M., and Hallquist, M.: Online gas-
671   and particle-phase measurements of organosulfates, organosulfonates and nitrooxy organosulfates in Beijing utilizing a

672   FIGAERO ToF-CIMS, Atmos. Chem. Phys., 18, 10355-10371, 10.5194/acp-18-10355-2018, 2018.

673   Lewandowski, M., Jaoui, M., Offenberg, J. H., Krug, J. D., and Kleindienst, T. E.: Atmospheric oxidation of isoprene and 1,3-
674   butadiene: influence of aerosol acidity and relative humidity on secondary organic aerosol, Atmos. Chem. Phys., 15, 3773-3783,
675   10.5194/acp-15-3773-2015, 2015.

676   Liao, J., Froyd, K. D., Murphy, D. M., Keutsch, F. N., Yu, G., Wennberg, P. O., St. Clair, J. M., Crounse, J. D., Wisthaler, A.,
677   Mikoviny, T., Jimenez, J. L., Campuzano-Jost, P., Day, D. A., Hu, W., Ryerson, T. B., Pollack, I. B., Peischl, J., Anderson, B. E.,
678   Ziemba, L. D., Blake, D. R., Meinardi, S., and Diskin, G.: Airborne measurements of organosulfates over the continental US, J.
679   Geophys. Res.-Atmos., 120, 2990-3005, 10.1002/2014jd022378, 2015.

680   Lin, P., Yu, J. Z., Engling, G., and Kalberer, M.: Organosulfates in humic-like substance fraction isolated from aerosols at seven
681   locations in East Asia: a study by ultra-high-resolution mass spectrometry, Environ. Sci. Technol., 46, 13118-13127,
682   10.1021/es303570v, 2012a.

683   Lin, Y. H., Zhang, Z., Docherty, K. S., Zhang, H., Budisulistiorini, S. H., Rubitschun, C. L., Shaw, S. L., Knipping, E. M., Edgerton,
684   E. S., Kleindienst, T. E., Gold, A., and Surratt, J. D.: Isoprene epoxydiols as precursors to secondary organic aerosol formation:
685   acid-catalyzed reactive uptake studies with authentic compounds, Environ. Sci. Technol., 46, 250-258, 10.1021/es202554c,
686   2012b.

687   Lin, Y. H., Zhang, H., Pye, H. O., Zhang, Z., Marth, W. J., Park, S., Arashiro, M., Cui, T., Budisulistiorini, S. H., Sexton, K. G.,
688   Vizuete, W., Xie, Y., Luecken, D. J., Piletic, I. R., Edney, E. O., Bartolotti, L. J., Gold, A., and Surratt, J. D.: Epoxide as a
689   precursor to secondary organic aerosol formation from isoprene photooxidation in the presence of nitrogen oxides, P. Natl. Acad.
690   Sci. USA, 110, 6718-6723, 10.1073/pnas.1221150110, 2013.

691   Liu, M. X., Song, Y., Zhou, T., Xu, Z. Y., Yan, C. Q., Zheng, M., Wu, Z. J., Hu, M., Wu, Y. S., and Zhu, T.: Fine particle pH during
692   severe haze episodes in northern China, Geophys. Res. Lett., 44, 5213-5221, 10.1002/2017gl073210, 2017.

693   Liu, Y., and Wang, T.: Worsening urban ozone pollution in China from 2013 to 2017-Part 2: The effects of emission changes and
694   implications for multi-pollutant control, Atmos. Chem. Phys., 20, 6323-6337, 10.5194/acp-20-6323-2020, 2020.

695   Lukacs, H., Gelencser, A., Hoffer, A., Kiss, G., Horvath, K., and Hartyani, Z.: Quantitative assessment of organosulfates in size-
696   segregated rural fine aerosol, Atmos. Chem. Phys., 9, 231-238, 10.5194/acp-9-231-2009, 2009.

697   Ma, Y., Xu, X., Song, W., Geng, F., and Wang, L.: Seasonal and diurnal variations of particulate organosulfates in urban Shanghai,
698   China, Atmos. Environ., 85, 152-160, 10.1016/j.atmosenv.2013.12.017, 2014.

699   Mahowald, N.: Aerosol indirect effect on biogeochemical cycles and climate, Science, 334, 794-796, 10.1126/science.1207374,
700   2011.

701   McNeill, V. F., Woo, J. L., Kim, D. D., Schwier, A. N., Wannell, N. J., Sumner, A. J., and Barakat, J. M.: Aqueous-phase secondary
702   organic aerosol and organosulfate formation in atmospheric aerosols: a modeling study, Environ. Sci. Technol., 46, 8075-8081,
703   10.1021/es3002986, 2012.

704   Meade, L. E., Riva, M., Blomberg, M. Z., Brock, A. K., Qualters, E. M., Siejack, R. A., Ramakrishnan, K., Surratt, J. D., and
705   Kautzman, K. E.: Seasonal variations of fine particulate organosulfates derived from biogenic and anthropogenic hydrocarbons
706   in the mid-Atlantic United States, Atmos. Environ., 145, 405-414, 10.1016/j.atmosenv.2016.09.028, 2016.

707   Nah, T., Guo, H. Y., Sullivan, A. P., Chen, Y. L., Tanner, D. J., Nenes, A., Russell, A., Ng, N. L., Huey, L. G., and Weber, R. J.:
708   Characterization of aerosol composition, aerosol acidity, and organic acid partitioning at an agriculturally intensive rural
709   southeastern US site, Atmos. Chem. Phys., 18, 11471-11491, 10.5194/acp-18-11471-2018, 2018.

710   Nestorowicz, K., Jaoui, M., Rudzinski, K. J., Lewandowski, M., Kleindienst, T. E., Spolnik, G., Danikiewicz, W., and Szmigielski,
711   R.: Chemical composition of isoprene SOA under acidic and non-acidic conditions: effect of relative humidity, Atmos. Chem.
712   Phys., 18, 18101-18121, 10.5194/acp-18-18101-2018, 2018.

713   Nguyen, Q. T., Christensen, M. K., Cozzi, F., Zare, A., Hansen, A. M. K., Kristensen, K., Tulinius, T. E., Madsen, H. H., Christensen,
714   J. H., Brandt, J., Massling, A., Nøjgaard, J. K., and Glasius, M.: Understanding the anthropogenic influence on formation of
715   biogenic secondary organic aerosols in Denmark via analysis of organosulfates and related oxidation products, Atmos. Chem.
716   Phys., 14, 8961-8981, 10.5194/acp-14-8961-2014, 2014.

717   Nguyen, T. B., Lee, P. B., Updyke, K. M., Bones, D. L., Laskin, J., Laskin, A., and Nizkorodov, S. A.: Formation of nitrogen- and
718   sulfur-containing light-absorbing compounds accelerated by evaporation of water from secondary organic aerosols, J. Geophys.
719   Res.-Atmos., 117, 10.1029/2011jd016944, 2012.

720   Nguyen, T. B., Bates, K. H., Crounse, J. D., Schwantes, R. H., Zhang, X., Kjaergaard, H. G., Surratt, J. D., Lin, P., Laskin, A.,
721   Seinfeld, J. H., and Wennberg, P. O.: Mechanism of the hydroxyl radical oxidation of methacryloyl peroxynitrate (MPAN) and
722   its pathway toward secondary organic aerosol formation in the atmosphere, Phys. Chem. Chem. Phys., 17, 17914-17926,
723   10.1039/c5cp02001h, 2015.

724   Nozière, B., Kaberer, M., Claeys, M., Allan, J., D'Anna, B., Decesari, S., Finessi, E., Glasius, M., Grgic, I., Hamilton, J. F., Hoffmann,
725   T., Iinuma, Y., Jaoui, M., Kahno, A., Kampf, C. J., Kourtchev, I., Maenhaut, W., Marsden, N., Saarikoski, S., Schnelle-Kreis, J.,
726   Surratt, J. D., Szidat, S., Szmigielski, R., and Wisthaler, A.: The molecular identification of organic compounds in the atmosphere:
727   state of the art and challenges, Chem. Rev., 115, 3919-3983, 10.1021/cr5003485, 2015.

728   Nozière, B., Ekström, S., Alsberg, T., and Holmström, S.: Radical-initiated formation of organosulfates and surfactants in
729   atmospheric aerosols, Geophys. Res. Lett., 37, 10.1029/2009gl041683, 2010.

730   Olson, C. N., Galloway, M. M., Yu, G., Hedman, C. J., Lockett, M. R., Yoon, T., Stone, E. A., Smith, L. M., and Keutsch, F. N.:
731   Hydroxycarboxylic acid-derived organosulfates: synthesis, stability, and quantification in ambient aerosol, Environ. Sci.
732   Technol., 45, 6468-6474, 10.1021/es201039p, 2011.

733   Olson, N. E., Lei, Z. Y., Craig, R. L., Zhang, Y., Chen, Y. Z., Lambe, A. T., Zhang, Z. F., Gold, A., Surratt, J. D., and Ault, A. P.:

734 Reactive uptake of isoprene epoxydiols increases the viscosity of the core of phase-separated aerosol particles, ACS Earth Space
735 Chem., 3, 1402-1414, 10.1021/acsearthspacechem.9b00138, 2019.
736 Passananti, M., Kong, L., Shang, J., Dupart, Y., Perrier, S., Chen, J., Donaldson, D. J., and George, C.: Organosulfate formation
737 through the heterogeneous reaction of sulfur dioxide with unsaturated fatty acids and long-chain alkenes, Angew. Chem. Int. Ed.
738 Engl., 55, 10336-10339, 10.1002/anie.201605266, 2016.
739 Pye, H. O. T., Pinder, R. W., Piletic, I. R., Xie, Y., Capps, S. L., Lin, Y. H., Surratt, J. D., Zhang, Z. F., Gold, A., Luecken, D. J.,
740 Hutzell, W. T., Jaoui, M., Offenberg, J. H., Kleindienst, T. E., Lewandowski, M., and Edney, E. O.: Epoxide pathways improve
741 model predictions of isoprene markers and reveal key role of acidity in aerosol formation, Environ. Sci. Technol., 47, 11056-
742 11064, 10.1021/es402106h, 2013.
743 Ramanathan, V., Crutzen, P. J., Lelieveld, J., Mitra, A. P., Althausen, D., Anderson, J., Andreae, M. O., Cantrell, W., Cass, G. R.,
744 Chung, C. E., Clarke, A. D., Coakley, J. A., Collins, W. D., Conant, W. C., Dulac, F., Heintzenberg, J., Heymsfield, A. J., Holben,
745 B., Howell, S., Hudson, J., Jayaraman, A., Kiehl, J. T., Krishnamurti, T. N., Lubin, D., McFarquhar, G., Novakov, T., Ogren, J.
746 A., Podgorny, I. A., Prather, K., Priestley, K., Prospero, J. M., Quinn, P. K., Rajeev, K., Rasch, P., Rupert, S., Sadourny, R.,
747 Satheesh, S. K., Shaw, G. E., Sheridan, P., and Valero, F. P. J.: Indian Ocean Experiment: an integrated analysis of the climate
748 forcing and effects of the great Indo-Asian haze, J. Geophys. Res.-Atmos., 106, 28371-28398, 10.1029/2001jd900133, 2001.
749 Rattanavaraha, W., Chu, K., Budisulistiorini, S. H., Riva, M., Lin, Y. H., Edgerton, E. S., Baumann, K., Shaw, S. L., Guo, H., King,
750 L., Weber, R. J., Neff, M. E., Stone, E. A., Offenberg, J. H., Zhang, Z., Gold, A., and Surratt, J. D.: Assessing the impact of
751 anthropogenic pollution on isoprene-derived secondary organic aerosol formation in $PM_{2.5}$ collected from the Birmingham,
752 Alabama, ground site during the 2013 Southern Oxidant and Aerosol Study, Atmos. Chem. Phys., 16, 4897-4914, 10.5194/acp-
753 16-4897-2016, 2017.
754 Riva, M., Tomaz, S., Cui, T., Lin, Y. H., Perraudin, E., Gold, A., Stone, E. A., Villenave, E., and Surratt, J. D.: Evidence for an
755 unrecognized secondary anthropogenic source of organosulfates and sulfonates: gas-phase oxidation of polycyclic aromatic
756 hydrocarbons in the presence of sulfate aerosol, Environ. Sci. Technol., 49, 6654-6664, 10.1021/acs.est.5b00836, 2015.
757 Riva, M., Budisulistiorini, S. H., Zhang, Z. F., Gold, A., and Surratt, J. D.: Chemical characterization of secondary organic aerosol
758 constituents from isoprene ozonolysis in the presence of acidic aerosol, Atmos. Environ., 130, 5-13,
759 10.1016/j.atmosenv.2015.06.027, 2016a.
760 Riva, M., Da Silva Barbosa, T., Lin, Y.-H., Stone, E. A., Gold, A., and Surratt, J. D.: Chemical characterization of organosulfates in
761 secondary organic aerosol derived from the photooxidation of alkanes, Atmos. Chem. Phys., 16, 11001-11018, 10.5194/acp-16-
762 11001-2016, 2016b.
763 Riva, M., Chen, Y., Zhang, Y., Lei, Z., Olson, N. E., Boyer, H. C., Narayan, S., Yee, L. D., Green, H. S., Cui, T., Zhang, Z., Baumann,
764 K., Fort, M., Edgerton, E., Budisulistiorini, S. H., Rose, C. A., Ribeiro, I. O., RL, E. O., Dos Santos, E. O., Machado, C. M. D.,
765 Szopa, S., Zhao, Y., Alves, E. G., de Sa, S. S., Hu, W., Knipping, E. M., Shaw, S. L., Duvoisin Junior, S., de Souza, R. A. F.,
766 Palm, B. B., Jimenez, J. L., Glasius, M., Goldstein, A. H., Pye, H. O. T., Gold, A., Turpin, B. J., Vizuete, W., Martin, S. T.,
767 Thornton, J. A., Dutcher, C. S., Ault, A. P., and Surratt, J. D.: Increasing Isoprene Epoxydiol-to-Inorganic Sulfate Aerosol Ratio
768 Results in Extensive Conversion of Inorganic Sulfate to Organosulfur Forms: Implications for Aerosol Physicochemical
769 Properties, Environ. Sci. Technol., 53, 8682-8694, 10.1021/acs.est.9b01019, 2019.
770 Schindelka, J., Iinuma, Y., Hoffmann, D., and Herrmann, H.: Sulfate radical-initiated formation of isoprene-derived organosulfates
771 in atmospheric aerosols, Faraday Discuss., 165, 237-259, 10.1039/c3fd00042g, 2013.
772 Shakya, K. M., and Peltier, R. E.: Investigating missing sources of sulfur at Fairbanks, Alaska, Environ. Sci. Technol., 47, 9332-
773 9338, 10.1021/es402020b, 2013.
774 Shakya, K. M., and Peltier, R. E.: Non-sulfate sulfur in fine aerosols across the United States: Insight for organosulfate prevalence,
775 Atmos. Environ., 100, 159-166, 10.1016/j.atmosenv.2014.10.058, 2015.
776 Shalamzari, M. S., Ryabtsova, O., Kahnt, A., Vermeylen, R., Herent, M. F., Quetin-Leclercq, J., Van der Veken, P., Maenhaut, W.,
777 and Claeys, M.: Mass spectrometric characterization of organosulfates related to secondary organic aerosol from isoprene, Rapid
778 Commun. Mass Spectrom., 27, 784-794, 10.1002/rcm.6511, 2013.
779 Shang, J., Passananti, M., Dupart, Y., Ciuraru, R., Tinel, L., Rossignol, S., Perrier, S., Zhu, T., and George, C.: SO_2 uptake on oleic
780 acid: a new formation pathway of organosulfur compounds in the atmosphere, Environ. Sci. Technol. Lett., 3, 67-72,
781 10.1021/acs.estlett.6b00006, 2016.
782 Shi, G. L., Xu, J., Peng, X., Xiao, Z. M., Chen, K., Tian, Y. Z., Guan, X. B., Feng, Y. C., Yu, H. F., Nenes, A., and Russell, A. G.:
783 aerosols in a polluted atmosphere: source contributions to highly acidic aerosol, Environ. Sci. Technol., 51, 4289-4296,
784 10.1021/acs.est.6b05736, 2017.
785 Shiraiwa, M., Ammann, M., Koop, T., and Poschl, U.: Gas uptake and chemical aging of semisolid organic aerosol particles, P. Natl.
786 Acad. Sci. USA, 108, 11003-11008, 10.1073/pnas.1103045108, 2011.
787 Shrivastava, M., Cappa, C. D., Fan, J. W., Goldstein, A. H., Guenther, A. B., Jimenez, J. L., Kuang, C., Laskin, A., Martin, S. T.,
788 Ng, N. L., Petaja, T., Pierce, J. R., Rasch, P. J., Roldin, P., Seinfeld, J. H., Shilling, J., Smith, J. N., Thornton, J. A., Volkamer,
789 R., Wang, J., Worsnop, D. R., Zaveri, R. A., Zelenyuk, A., and Zhang, Q.: Recent advances in understanding secondary organic
790 aerosol: Implications for global climate forcing, Rev. Geophys., 55, 509-559, 2017.
791 Song, S., Nenes, A., Gao, M., Zhang, Y., Liu, P., Shao, J., Ye, D., Xu, W., Lei, L., Sun, Y., Liu, B., Wang, S., and McElroy, M. B.:
792 Thermodynamic modeling suggests declines in water uptake and acidity of inorganic aerosols in Beijing winter haze events
793 during 2014/2015-2018/2019, Environ. Sci. Technol. Lett., 6, 752-760, 10.1021/acs.estlett.9b00621, 2019.
794 Staudt, S., Kundu, S., Lehmler, H. J., He, X., Cui, T., Lin, Y. H., Kristensen, K., Glasius, M., Zhang, X., Weber, R. J., Surratt, J. D.,
795 and Stone, E. A.: Aromatic organosulfates in atmospheric aerosols: synthesis, characterization, and abundance, Atmos. Environ.,

94, 366-373, 10.1016/j.atmosenv.2014.05.049, 2014.

Stone, E. A., Yang, L., Yu, L. E., and Rupakheti, M.: Characterization of organosulfates in atmospheric aerosols at Four Asian locations, Atmos. Environ., 47, 323-329, 10.1016/j.atmosenv.2011.10.058, 2012.

Surratt, J. D., Kroll, J. H., Kleindienst, T. E., Edney, E. O., Claeys, M., Sorooshian, A., Ng, N. L., Offenberg, J. H., Lewandowski, M., Jaoui, M., Flagan, R. C., and Seinfeld, J. H.: Evidence for organosulfates in secondary organic aerosol, Environ. Sci. Technol., 41, 517-527, 10.1021/es062081q, 2007a.

Surratt, J. D., Lewandowski, M., Offenberg, J. H., Jaoui, M., Kleindienst, T. E., Edney, E. O., and Seinfeld, J. H.: Effect of acidity on secondary organic aerosol formation from isoprene, Environ. Sci. Technol., 41, 5363-5369, 10.1021/es0704176, 2007b.

Surratt, J. D., Gómez-González, Y., Chan, A. W. H., Vermeylen, R., Shahgholi, M., Kleindienst, T. E., Edney, E. O., Offenberg, J. H., Lewandowski, M., Jaoui, M., Maenhaut, W., Claeys, M., Richard C. Flagan, and Seinfeld, J. H.: Organosulfate formation in biogenic secondary organic aerosol, J. Phys. Chem. A, 8345–8378, 2008.

Surratt, J. D., Chan, A. W., Eddingsaas, N. C., Chan, M., Loza, C. L., Kwan, A. J., Hersey, S. P., Flagan, R. C., Wennberg, P. O., and Seinfeld, J. H.: Reactive intermediates revealed in secondary organic aerosol formation from isoprene, P. Natl. Acad. Sci. USA, 107, 6640-6645, 10.1073/pnas.0911114107, 2010.

Tao, J., Zhang, L., Cao, J., and Zhang, R.: A review of current knowledge concerning $PM_{2.5}$ chemical composition, aerosol optical properties and their relationships across China, Atmos. Chem. Phys., 17, 9485-9518, 10.5194/acp-17-9485-2017, 2017.

Tao, S., Lu, X., Levac, N., Bateman, A. P., Nguyen, T. B., Bones, D. L., Nizkorodov, S. A., Laskin, J., Laskin, A., and Yang, X.: Molecular characterization of organosulfates in organic aerosols from Shanghai and Los Angeles urban areas by nanospray-desorption electrospray ionization high-resolution mass spectrometry, Environ. Sci. Technol., 48, 10993-11001, 10.1021/es5024674, 2014.

Tolocka, M. P., and Turpin, B.: Contribution of organosulfur compounds to organic aerosol mass, Environ. Sci. Technol., 46, 7978-7983, 10.1021/es300651v, 2012.

Wach, P., Spolnik, G., Rudzinski, K. J., Skotak, K., Claeys, M., Danikiewicz, W., and Szmigielski, R.: Radical oxidation of methyl vinyl ketone and methacrolein in aqueous droplets: characterization of organosulfates and atmospheric implications, Chemosphere, 214, 1-9, 10.1016/j.chemosphere.2018.09.026, 2019.

Wang, H. C., Chen, X. R., Lu, K. D., Hu, R. Z., Li, Z. Y., Wang, H. L., Ma, X. F., Yang, X. P., Chen, S. Y., Dong, H. B., Liu, Y., Fang, X., Zeng, L. M., Hu, M., and Zhang, Y. H.: NO_3 and N_2O_5 chemistry at a suburban site during the EXPLORE-YRD campaign in 2018, Atmos. Environ., 224, 10.1016/j.atmosenv.2019.117180, 2020a.

Wang, H. L., Qiao, L. P., Lou, S. R., Zhou, M., Ding, A. J., Huang, H. Y., Chen, J. M., Wang, Q., Tao, S. K., Chen, C. H., Li, L., and Huang, C.: Chemical composition of $PM_{2.5}$ and meteorological impact among three years in urban Shanghai, China, J. Clean Prod., 112, 1302-1311, 10.1016/j.jclepro.2015.04.099, 2016a.

Wang, J. J., Lu, X. M., Yan, Y. T., Zhou, L. G., and Ma, W. C.: Spatiotemporal characteristics of $PM_{2.5}$ concentration in the Yangtze River Delta urban agglomeration, China on the application of big data and wavelet analysis, Sci. Total Environ., 724, 10.1016/j.scitotenv.2020.138134, 2020b.

Wang, K., Zhang, Y., Huang, R. J., Wang, M., Ni, H., Kampf, C. J., Cheng, Y., Bilde, M., Glasius, M., and Hoffmann, T.: Molecular characterization and source identification of atmospheric particulate organosulfates using ultrahigh resolution mass spectrometry, Environ. Sci. Technol., 53, 6192-6202, 10.1021/acs.est.9b02628, 2019a.

Wang, S. Y., Zhou, S. M., Tao, Y., Tsui, W. G., Ye, J. H., Yu, J. Z., Murphy, J. G., McNeill, V. F., Abbatt, J. P. D., and Chan, A. W. H.: Organic peroxides and sulfur dioxide in aerosol: source of particulate sulfate, Environ. Sci. Technol., 53, 10695-10704, 10.1021/acs.est.9b02591, 2019b.

Wang, X. K., Rossignol, S., Ma, Y., Yao, L., Wang, M. Y., Chen, J. M., George, C., and Wang, L.: Molecular characterization of atmospheric particulate organosulfates in three megacities at the middle and lower reaches of the Yangtze River, Atmos. Chem. Phys., 16, 2285-2298, 10.5194/acp-16-2285-2016, 2016b.

Wang, Y., Ren, J., Huang, X. H. H., Tong, R., and Yu, J. Z.: Synthesis of four monoterpene-derived organosulfates and their quantification in atmospheric aerosol samples, Environ. Sci. Technol., 51, 6791-6801, 10.1021/acs.est.7b01179, 2017.

Wang, Y., Hu, M., Guo, S., Wang, Y., Zheng, J., Yang, Y., Zhu, W., Tang, R., Li, X., Liu, Y., Le Breton, M., Du, Z., Shang, D., Wu, Y., Wu, Z., Song, Y., Lou, S., Hallquist, M., and Yu, J.: The secondary formation of organosulfates under interactions between biogenic emissions and anthropogenic pollutants in summer in Beijing, Atmos. Chem. Phys., 18, 10693-10713, 10.5194/acp-18-10693-2018, 2018.

Wen, L., Xue, L. K., Wang, X. F., Xu, C. H., Chen, T. S., Yang, L. X., Wang, T., Zhang, Q. Z., and Wang, W. X.: Summertime fine particulate nitrate pollution in the North China Plain: increasing trends, formation mechanisms and implications for control policy, Atmos. Chem. Phys., 18, 11261-11275, 10.5194/acp-18-11261-2018, 2018.

Worton, D. R., Surratt, J. D., Lafranchi, B. W., Chan, A. W., Zhao, Y., Weber, R. J., Park, J. H., Gilman, J. B., de Gouw, J., Park, C., Schade, G., Beaver, M., Clair, J. M., Crounse, J., Wennberg, P., Wolfe, G. M., Harrold, S., Thornton, J. A., Farmer, D. K., Docherty, K. S., Cubison, M. J., Jimenez, J. L., Frossard, A. A., Russell, L. M., Kristensen, K., Glasius, M., Mao, J., Ren, X., Brune, W., Browne, E. C., Pusede, S. E., Cohen, R. C., Seinfeld, J. H., and Goldstein, A. H.: Observational insights into aerosol formation from isoprene, Environ. Sci. Technol., 47, 11403-11413, 10.1021/es4011064, 2013.

Yao, M., Zhao, Y., Hu, M., Huang, D., Wang, Y., Yu, J. Z., and Yan, N.: Multiphase reactions between secondary organic aerosol and sulfur dioxide: kinetics and contributions to sulfate formation and aerosol aging, Environ. Sci. Technol. Lett., 6, 768-774, 10.1021/acs.estlett.9b00657, 2019.

Yassine, M. M., Dabek-Zlotorzynska, E., Harir, M., and Schmitt-Kopplin, P.: Identification of weak and strong organic acids in atmospheric aerosols by capillary electrophoresis/mass spectrometry and ultra-high-resolution fourier transform ion cyclotron

858 resonance mass spectrometry, Anal. Chem., 84, 6586-6594, 10.1021/ac300798g, 2012.

859 Zhang, H., Worton, D. R., Lewandowski, M., Ortega, J., Rubitschun, C. L., Park, J. H., Kristensen, K., Campuzano-Jost, P., Day, D.
860 A., Jimenez, J. L., Jaoui, M., Offenberg, J. H., Kleindienst, T. E., Gilman, J., Kuster, W. C., de Gouw, J., Park, C., Schade, G.
861 W., Frossard, A. A., Russell, L., Kaser, L., Jud, W., Hansel, A., Cappellin, L., Karl, T., Glasius, M., Guenther, A., Goldstein, A.
862 H., Seinfeld, J. H., Gold, A., Kamens, R. M., and Surratt, J. D.: Organosulfates as tracers for secondary organic aerosol (SOA)
863 formation from 2-methyl-3-buten-2-ol (MBO) in the atmosphere, Environ. Sci. Technol., 46, 9437-9446, 10.1021/es301648z,
864 2012.

865 Zhang, H., Zhang, Z., Cui, T., Lin, Y. H., Bhathela, N. A., Ortega, J., Worton, D. R., Goldstein, A. H., Guenther, A., Jimenez, J. L.,
866 Gold, A., and Surratt, J. D.: Secondary organic aerosol formation via 2-methyl-3-buten-2-ol photooxidation: evidence of acid-
867 catalyzed reactive uptake of epoxides, Environ. Sci. Technol. Lett., 1, 242-247, 10.1021/ez500055f, 2014.

868 Zheng, G., Su, H., Wang, S., Andreae, M. O., Poschl, U., and Cheng, Y.: Multiphase buffer theory explains contrasts in atmospheric
869 aerosol acidity, Science, 369, 1374-1377, 10.1126/science.aba3719, 2020.

870 Zhu, M., Jiang, B., Li, S., Yu, Q., Yu, X., Zhang, Y., Bi, X., Yu, J., George, C., Yu, Z., and Wang, X.: Organosulfur compounds

871 formed from heterogeneous reaction between SO2 and particulate-bound unsaturated fatty acids in ambient air, Environ. Sci.

872 Technol. Lett., 6, 318-322, 10.1021/acs.estlett.9b00218, 2019.

873

874

875 **Table 1.** Organosulfates (in ng m^{-3}) quantified by UPLC-ESI(-)-QToFMS.

Category	m/z, [M-H]$^-$	Formula, [M-H]$^-$	Retention time	Standards for quantification	Proposed structure	Ref.	Average concentration	
							2015/2016	2018/2019
	167.0014	C$_4$H$_7$O$_5$S$^-$	0.85,1.36	Lactic acid sulfate (LAS)		a	1.13	1.45
	182.9963	C$_4$H$_7$O$_6$S$^-$	0.78,2.23	LAS		b	2.84	2.19
	197.0120	C$_5$H$_9$O$_6$S$^-$	0.85,1.55,3.11,3.99	LAS		c	1.87	1.72
	198.9912	C$_4$H$_7$O$_7$S$^-$	0.74,3.86	LAS		d	2.28	2.50
	199.0276	C$_5$H$_{11}$O$_6$S$^-$	0.85,8.08	LAS		c	0.57	0.65
	210.9912	C$_5$H$_7$O$_7$S$^-$	0.77	LAS		d	6.09	4.81
Isoprene OS	213.0069	C$_5$H$_9$O$_7$S$^-$	0.84	LAS		d	3.81	3.82
	215.0226	C$_5$H$_{11}$O$_7$S$^-$	0.72	LAS		e	11.35	8.92
	237.0069	C$_7$H$_9$O$_7$S$^-$	0.87,1.5	LAS		f	0.58	0.50
	260.0076	C$_5$H$_{10}$NO$_9$S$^-$	1.19	LAS		g	2.28	2.96
	273.9869	C$_5$H$_8$NO$_{10}$S$^-$	1.3	LAS		h	1.89	4.87
	223.0276	C$_7$H$_{11}$O$_6$S$^-$	2.52,2.87,3.19,3.42	Glycolic acid sulfate (GAS)		i	1.37	1.12
	239.0225	C$_7$H$_{11}$O$_7$S$^-$	0.85,1.77,2.03,3.08	GAS		f	1.91	2.01
	249.0797	C$_{10}$H$_{17}$O$_5$S$^-$	5.34,5.60,6.85,7.04, 7.12,7.36	α-Pinene sulfate		j	0.33	0.17
	251.0589	C$_9$H$_{15}$O$_6$S$^-$	3.63,4.14,4.82,7.35	Limonaketone sulfate		j	1.32	1.02
Monoterpene OS	253.0382	C$_8$H$_{13}$O$_7$S$^-$	3.35,3.63,4.45	GAS		a	1.39	1.73
	279.0538	C$_{10}$H$_{15}$O$_7$S$^-$	3.42,4.34,4.55,4.71	GAS		g	2.99	4.00
	281.0695	C$_{10}$H$_{17}$O$_7$S$^-$	4.93,5.14	α-Pinene sulfate		f	0.34	0.21
	294.0648	C$_{10}$H$_{16}$NO$_7$S$^-$	8.14,9.02,9.16,9.35	α-Pinene sulfate		k	6.21	5.55

	m/z	Formula	Retention times*	Name	Structure	Ref	2015/2016	2018/2019
	296.0440	$C_9H_{14}NO_8S^-$	4.72,4.86,5.24,6.44	Limonaketone sulfate		k	1.62	2.29
	342.0495	$C_{10}H_{16}NO_{10}S^-$	4.57,4.71,5.17,7.35	Limonaketone sulfate		i	1.32	1.59
Anthropogenic OS	151.0065	$C_4H_7O_4S^-$	0.92,2.87,4.11,5.23, 5.39,8.21	Methyl sulfate	unknown	–	2.04	1.80
	194.9963	$C_5H_7O_6S^-$	0.82,2.86	GAS	unknown	–	0.83	0.76
	209.0120	$C_6H_9O_6S^-$	0.87,2.09,3.27,4.06	GAS	unknown	–	1.44	0.63
	209.0845	$C_8H_{17}O_4S^-$	9.64	Sodium octyl sulfate		–	1.04	0.86
	172.9909	$C_6H_5O_4S^-$	2.6	Phenyl sulfate		l	0.36	0.12
	187.0065	$C_7H_7O_4S^-$	4.54	Phenyl sulfate		l	0.35	0.17
C₂/C₃ OS	136.9909	$C_3H_5O_4S^-$	0.78,3.93	GAS	unknown	–	0.62	0.50
	138.9701	$C_2H_3O_5S^-$	0.69	GAS		g	0.58	0.57
	152.9858	$C_3H_5O_5S^-$	0.81	GAS		d	2.30	1.79
	154.9650	$C_2H_3O_6S^-$	0.69	GAS		m	2.91	2.25
	155.0014	$C_3H_7O_5S^-$	0.79	GAS		n	1.21	0.70
	168.9807	$C_3H_5O_6S^-$	0.82	LAS		m	2.24	1.94
Unknown source OS	164.9858	$C_4H_5O_5S^-$	0.79	Methyl sulfate		n	1.20	0.78
	241.9971	$C_5H_8NO_8S^-$	3.39,3.57,3.93,4.21	Methyl sulfate		n	1.67	1.21
SUM							**65.48**	**59.04**

876 *Retention times of each OS isomer considered in the quantification. References for proposed OS structures: [a] Schindelka et
877 al. (2013)), [b] Shalamzari et al. (2013), [c] Riva et al. (2016a), [d] Hettiyadura et al. (2015), [e] Surratt et al. (2010), [f] Nozière et al.
878 (2010), [g] (Surratt et al., 2007a) , [h] Nestorowicz et al. (2018), [i] Yassine et al. (2012), [j] Wang et al. (2017), [k] Surratt et al. (2008),
879 [l] Huang et al. (2018), [m] Olson et al. (2011), [n] Hettiyadura et al. (2019).

880

881

882

883 **Table 2.** A summary of OS concentration (in ng m^{-3}) and its contribution to OM (OS/OM) in four seasons in 2015/2016 and
884 2018/2019.

Season	2015/2016		2018/2019	
	OS	OS/OM	OS	OS/OM
All year	65.5±77.5	0.57%±0.56%	59.4±79.7	0.66%±0.56%
Spring	51.1±24.4	0.34%±0.10%	51.5±28.8	0.48%±0.15%
Summer	114.1±128.4	1.13%±0.78%	102.1±137.7	1.18%±0.81%
Autumn	38.2±21.7	0.36%±0.11%	38.0±20.0	0.54%±0.24%
Winter	44.5±17.5	0.32%±0.12%	37.3±18.4	0.36%±0.13%

885
886

887
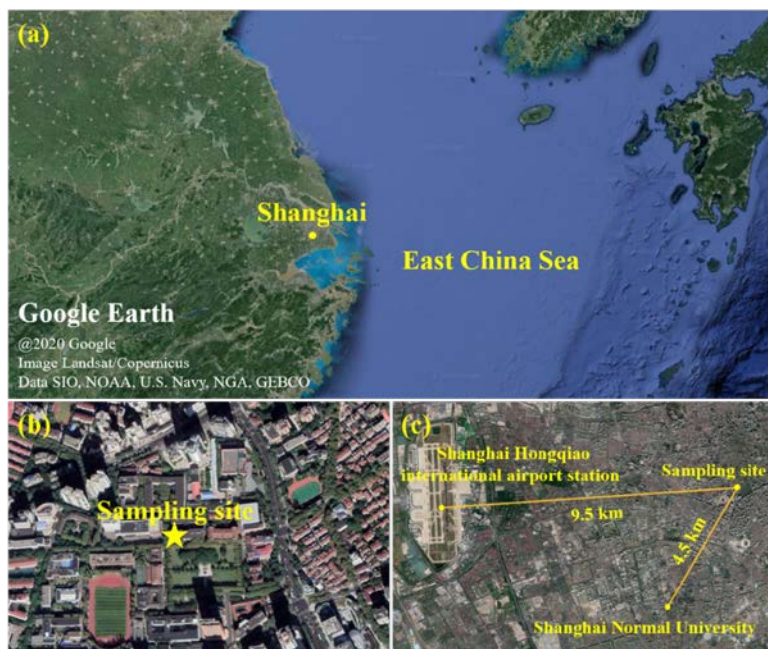
Figure 1. (a) Map of Shanghai. **(b)** Map of the sampling site on the Xuhui Campus of Shanghai Jiao Tong University in

downtown at 31.201^{o}N, 121.429^{o}E. **(c)** Map of the PM$_{2.5}$ sampling site, the meteorological station at Shanghai Hongqiao

international airport, the air quality monitoring station at Shanghai Normal University, and distances between them.

891
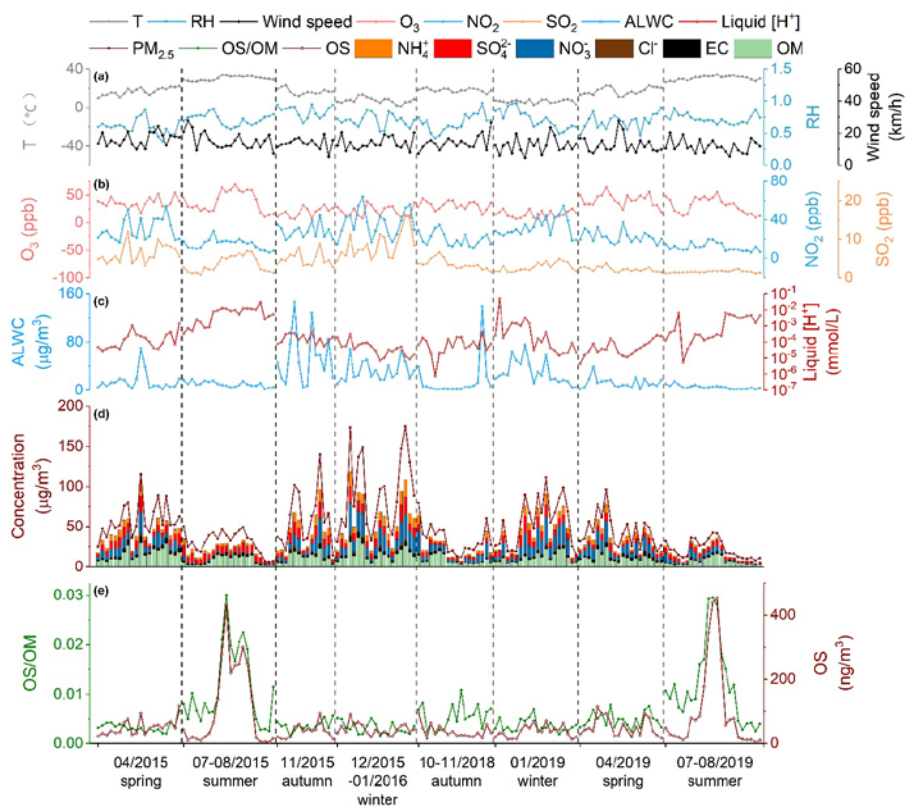
Figure 2. Time series of temperature, relative humid (RH), wind speed, O_3, NO_2, SO_2, aerosol liquid water content (ALWC)

893 and liquid [H^+], concentrations of particulate organic matter (OM), elemental carbon (EC), sulfate, nitrate, chloride,

894 ammonium, as well as the abundance of OS and its contribution to OM in 2015/2016 and 2018/2019 in Shanghai.
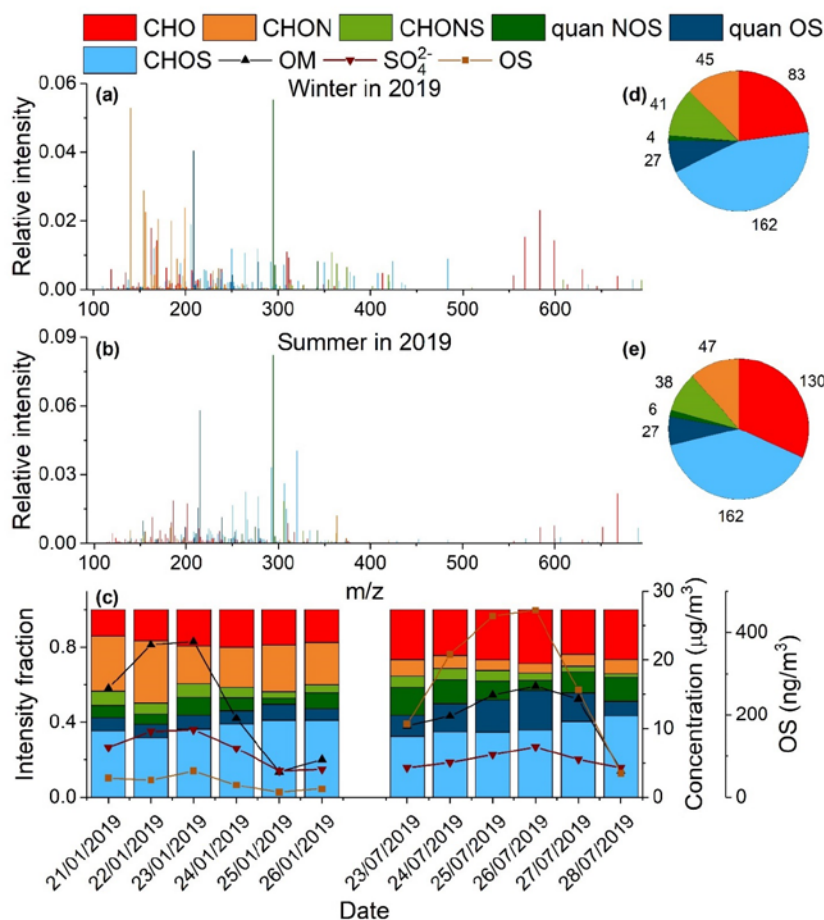
Figure 3. Average mass spectra of detected compounds in ambient aerosols during typical **(a)** wintertime (21-26 January 2019) and **(b)** summertime (23-28 July 2019) pollution episodes in Shanghai. The detected compounds were classified into six categories, i.e., CHO, CHON, CHOS, CHONS, quantified NOS, and quantified OS. The CHOS and CHONS categories excluded quantified OS and NOS, respectively. **(c)** The intensity fraction of different compound categories, as well as the time series of OM, SO_4^{2-}, and OS concentrations during two pollution episodes in 2019. **(d) (e)** The number of compounds detected in each category during the pollution episodes in winter and summer, respectively.
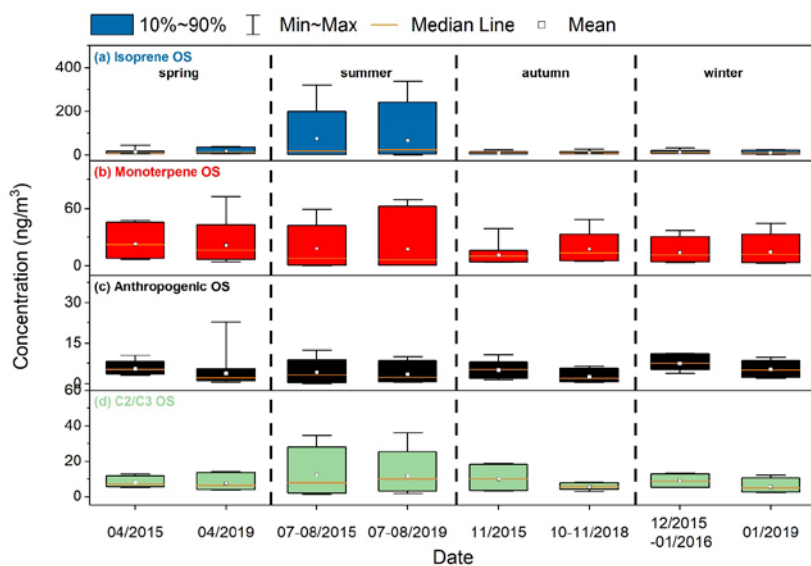
905
906 **Figure 4.** The concentrations of different types of the quantified OS over four seasons in 2015/2016 and 2018/2019.
907
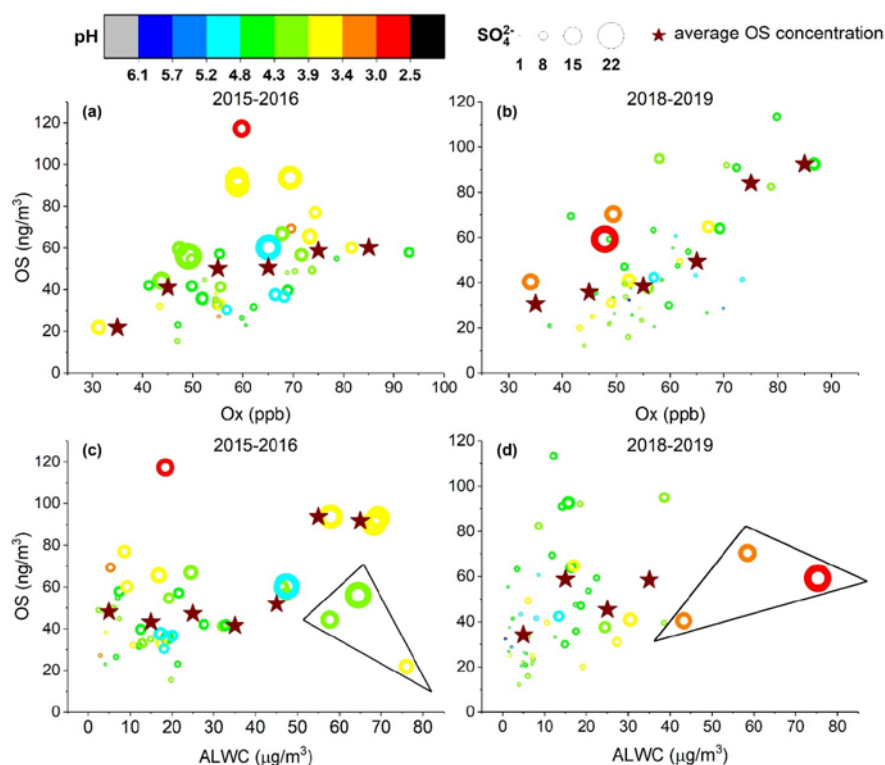
Figure 5. The quantified OS concentrations as a function of **(a) (b)** the level of O_x ($O_x = O_3 + NO_2$)level and **(c)(d)** aerosol liquid water content (ALWC) in 2015/2016 and 2018/2019 except for summer. The circles are colored according to the aerosol pH, and their size is linearly scaled with the SO_4^{2-} concentration. The Ox means the sum of O_3 and NO_2.The markers inside the triangle indicate the observations with low O_x levels (<50 ppb). The measured OS concentrations within regular O_x or ALWC intervals (every ten unit-length) were averaged to more obviously demonstrate the trend (star symbols).

914
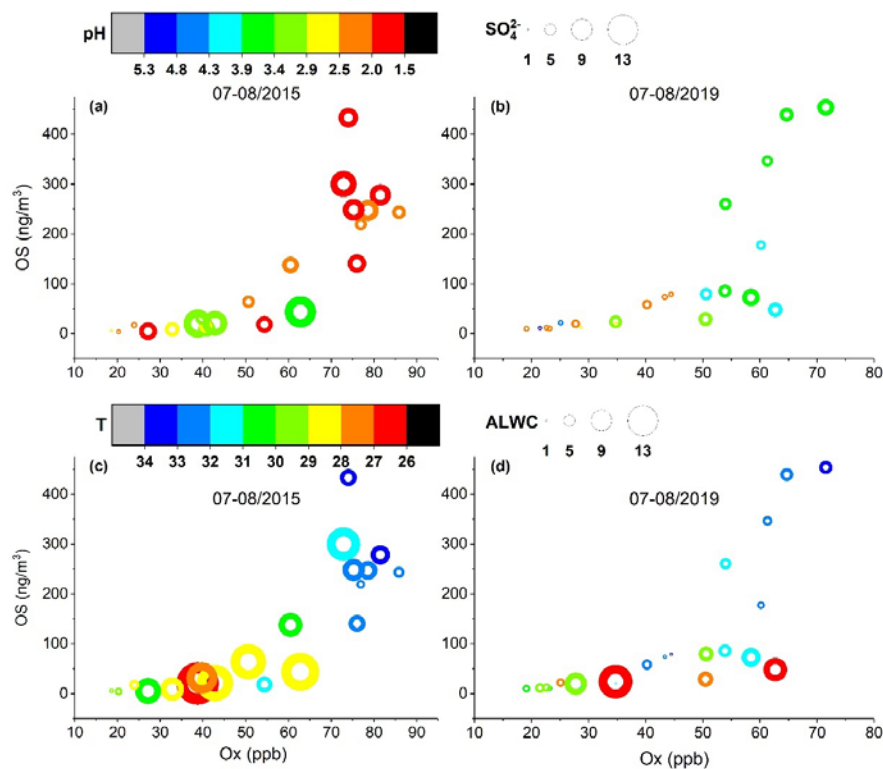
Figure 6. The quantified OS concentrations as a function of the Ox level in the summer of **(a) (c)** 2015 and **(b) (d)** 2019. The color of circles in **(a) (b)** indicates the aerosol pH, and their size is linearly scaled with the SO_4^{2-} concentration. The color of circles in **(c) (d)** indicates ambient temperature and their size is linearly scaled with aerosol liquid water content (ALWC).

918

919